Accepted Manuscript

Mobilization with granulocyte colony-stimulating factor blocks medullar erythropoiesis by depleting F4/80$^+$VCAM1$^+$CD169$^+$ER-HR3$^+$Ly6G$^+$ erythroid island macrophages in the mouse

Rebecca N. Jacobsen, Catherine E. Forristal, Liza J. Raggatt, Bianca Nowlan, Valerie Barbier, Simranpreet Kaur, Nico van Rooijen, Ingrid G. Winkler, Allisson R. Pettit, Jean-Pierre Levesque

PII: S0301-472X(14)00139-8

DOI: 10.1016/j.exphem.2014.03.009

Reference: EXPHEM 3118

To appear in: *Experimental Hematology*

Received Date: 20 December 2013

Revised Date: 25 March 2014

Accepted Date: 31 March 2014

Please cite this article as: Jacobsen RN, Forristal CE, Raggatt LJ, Nowlan B, Barbier V, Kaur S, van Rooijen N, Winkler IG, Pettit AR, Levesque J-P, Mobilization with granulocyte colony-stimulating factor blocks medullar erythropoiesis by depleting F4/80$^+$VCAM1$^+$CD169$^+$ER-HR3$^+$Ly6G$^+$ erythroid island macrophages in the mouse, *Experimental Hematology* (2014), doi: 10.1016/j.exphem.2014.03.009.

Mobilization with granulocyte colony-stimulating factor blocks medullar erythropoiesis by depleting F4/80$^+$VCAM1$^+$CD169$^+$ER-HR3$^+$Ly6G$^+$ erythroid island macrophages in the mouse

Rebecca N Jacobsen[a,d], Catherine E Forristal[a], Liza J Raggatt[b], Bianca Nowlan[a], Valerie Barbier[c], Simranpreet Kaur[b], Nico van Rooijen[e], Ingrid G Winkler[c], Allisson R Pettit[b], Jean-Pierre Levesque[a,d]

[a]Stem Cell Biology Group, [b]Bones and Immunology Group, and [c]Stem Cells and Cancer Group, Mater Research Institute – University of Queensland, Woolloongabba, Queensland, Australia; [d]School of Medicine, University of Queensland, Saint Lucia, Queensland, Australia; [e]Department of Molecular Cell Biology, Vrije Universiteit, Amsterdam, The Netherlands.

Corresponding authors:

Jean-Pierre Levesque
Mater Research Intitute – The University of Queensland
Translational Research Institute
37 Kent Street
Woolloongabba, 4102
Phone: +61 7 3443 7571
Fax: +61 7 3163 2550
Email: jp.levesque@mater.uq.edu.au

Allison R Pettit
Mater Research Intitute – The University of Queensland
Translational Research Institute
37 Kent Street
Woolloongabba, 4102
Phone: +61 7 3443 7571
Fax: +61 7 3163 2550
Email: apettit@mmri.mater.org.au

ABSTRACT

Similar to other tissues, the bone marrow (BM) contains subsets of resident tissue macrophages which are essential to maintain bone formation, functional hematopoietic stem cell (HSC) niches, and erythropoiesis. Pharmacological doses of granulocyte colony-stimulating factor (G-CSF) mobilize HSC in part by interfering with HSC niche-supportive function of BM resident macrophages. As BM macrophages are key to both maintenance of HSC within their niche and erythropoiesis, we investigated the effect of mobilizing doses of G-CSF on erythropoiesis in mice. We now report that G-CSF blocks medullar erythropoiesis by depleting erythroid island macrophages we identified as co-expressing F4/80, vascular cell adhesion molecule (VCAM)-1, CD169, Ly-6G and the ER-HR3 erythroid island macrophage antigen. Broad macrophage depletion by injecting clodronate-loaded liposomes, or selective depletion of $CD169^+$ macrophages, also concomitantly depleted $F4/80^+VCAM\text{-}1^+CD169^+ER\text{-}HR3^+Ly\text{-}6G^+$ erythroid island macrophages and blocked erythropoiesis. This more precise phenotypic definition of erythroid island macrophages will enable studies on their biology and function in normal setting and diseases associated with anemia. Finally this study further illustrates that macrophages are potent relay of innate immunity and inflammation on bone, hematopoietic and erythropoietic maintenance and agents that affect these macrophages, such as G-CSF, are likely to affect these three processes concomitantly.

Introduction

Erythropoiesis, the processes leading to the formation of blood erythrocytes, is a highly active, life sustaining processes. Blood erythrocytes have a life span of 100-120 days and as such, a typical adult must produce 2.5 million erythrocytes per second to replace them. Erythropoiesis involves the differentiation of hematopoietic stem cells (HSCs) into myeloid-erythroid progenitors in the bone marrow (BM), which further commit to the erythroid lineage throughout the generation of proerythroblasts and erythroblasts. After synthesizing large quantities of hemoglobin, the final stages of erythroblast maturation involves extrusion of the nucleus to form anuclear reticulocytes, which then change shape in the blood to fully matured erythrocytes. Microscopy sections of BM have revealed that maturing erythroblasts rosette around a central macrophage to form erythroid islands[1-5]. It has been proposed that these erythroid island macrophages contribute to the efficient transport of iron to erythroblasts[2, 6] enabling the synthesis of large quantities of hemoglobin as O_2 and CO_2 transport which depends on Fe^{2+} complexed in the heme molecule. These "nursing" macrophages at the center of erythropoietic islands have also been proposed to secrete cytokines essential to erythroblast survival and maintenance such as insulin-like growth factor 1[7, 8]. Finally erythroid island macrophages phagocytose and degrade erythroblast nuclei during nuclear extrusion, a step necessary to generate anucleated reticulocytes[9, 10]. While these macrophages are essential for erythropoiesis, little work has been done on their phenotypic identification so they can be studied further, particularly in disease states where erythropoiesis is perturbed such as myelodysplastic syndrome, chronic and acute myeloid leukemia, and chronic inflammation.

Systemic administration of granulocyte-colony stimulating factor (G-CSF) mobilizes HSC from the BM into the blood in order to harvest large quantities of HSC for subsequent transplantation in humans. G-CSF causes HSC mobilization by perturbing HSC niches in the BM[11, 12]. This results in the down-regulation of cell adhesion molecules such as vascular cell adhesion molecule-1 (VCAM-1) and the chemokine CXC-motif ligand-12 (CXCL12), which are both essential to HSC retention within the BM[13-16]. Furthermore it has been recently demonstrated that this effect of G-CSF on HSC niches is mediated in part by a subset of BM macrophages[15-17]. In the mouse HSC niche supportive macrophages express the macrophage-specific antigen F4/80 together with the Ly-6G granulocyte antigen[16, 18]. A separate report suggests that HSC niche supportive macrophages express CD169 also called

sialic acid binding immunoglobulin-like lectin 1 (Siglec-1) or sialoadhesin[15]. However whether F4/80^{+}Ly-6G^{+} macrophages express CD169 has never been reported. G-CSF treatment depletes F4/80^{+}Ly-6G^{+} macrophages in the BM[16, 18], resulting in a concomitant loss of osteoblasts and bone formation, decreased expression of VCAM-1 and CXCL12, and HSC mobilization[15-17]. In support of this notion, three independent models of macrophage depletion result in HSPC mobilization in the mouse: 1) in macrophage Fas-induced apoptosis (MAFIA) transgenic mice, 2) by injection of clodronate-loaded liposomes into wild-type mice, or 3) following selective depletion of CD169^{+} macrophages in *Siglec1*$^{DTR/+}$ mice[15, 16]. Considering that macrophages are important regulators of both HSC niches and erythropoiesis, we explored the effect of mobilizing doses of G-CSF on erythropoiesis and erythroid island macrophages.

Materials and Methods

Mice and treatments

All procedures had been approved by the Animal Experimentation Ethics Committee of the University of Queensland.

C57BL/6 mice were purchased from the Animal Resource Centre (Perth, Australia). *Siglec1*$^{DTR/DTR}$ mice were obtained from the Riken Bio Resource Centre (Japan) and were bred with wild-type C57BL/6 females to generate *Siglec1*$^{DTR/+}$ mice for experimentations. Insertion of the simian diphtheria toxin receptor (DTR) into the *Siglec1* gene was detected by genomic PCR on ear clips using *Siglec1* forward primer 5'-CAATTTCCGGTGCTTACGGTG-3', *Siglec1* reverse primer 5'-CATAGTCTAGGCTTCTGTGC-3', and DTR primer 5'-CCGGAGCTCCTTCACATATTTGC-3' with an annealing temperature of 60°C giving 530bp and 788bp bands for *Siglec1* wild-type and *Siglec1*^{DTR} alleles respectively[19].

All experimentations were performed on 8-10 week old male mice. Mice were injected twice daily subcutaneously with 125µg/kg per injection recombinant human G-CSF (Neupogen, Amgen Thousand Oaks, CA) diluted in saline for injection or saline for up to 4 consecutive days.

For macrophage depletion, dichloromethylene bisphosphonate (clodronate, Roche Diagnostics, Mannheim, Germany) was packaged into liposomes as previously described [20]. Empty liposomes were prepared in the same conditions in PBS without clodronate. Phagocytic macrophages were depleted in vivo by retro-orbitally injecting 200µL/20g body

weight clodronate-loaded liposome suspension every second day. Control mice were injected with an equivalent volume of saline or PBS-loaded liposomes.

For selective CD169^{+} macrophage depletion, *Siglec1*$^{DTR/+}$ mice and control C57BL/6 wild-type mice were injected intraperitoneally daily with 10µg/kg purified diphtheria toxin DPT (MBL International).diluted in saline for injection

Tissue sampling

Mice were anesthetized and 1mL blood collected into heparinized tubes by cardiac exsanguinations. Spleens were harvested, weighed and dissociated in 3mL Iscove modified Dulbecco's medium (IMDM) with 10% FCS using a GentleMACS Dissociator tissue homogenizer with matching C tubes (Miltenyi Biotec) on "spleen 3" setting, twice. Femurs were cleaned of any remaining muscles with a scalpel and paper towel, BM cells were flushed out using a 21-gauge needle and a 1mL syringe containing 1mL PBS with 2% FCS. BM leukocytes were dissociated by successive pipetting with the mounted syringe.

Flow cytometry

BM cells and splenocytes were pelleted at 370xg for 5 minutes at 4°C and resuspended in CD16/CD32 hybridoma 2.4G2 supernatant. For macrophage staining, cells were stained with CD11b-Billiant Violet 605, anti-F4/80-AlexaFluor647 (clone CI:A3-1), anti-Ly-6G-PECY7 (clone 1A8), anti-VCAM-1-Pacific Blue (clone 429), CD169-FITC (clone 3D6.112), biotinylated ER-HR3 antibody, and streptavidin-PE.

For red cell staining, cells were stained with Ter119-FITC, CD71-PE and 50 µM Hoescht33342.

For erythroid island macrophage staining, femurs were split in halves lengthwise by poking nicks in the bone surface with a scalpel blade. The exposed BM was then gently removed from the opened bone with Iscove modified Dulbecco's medium supplemented with 10% FCS and a 1ml tip pipette in order to minimize disruption of cell aggregates. Cell suspension was then gently pipetted approximately 10 times and then resuspended in CD16/CD32 hybridoma 2.4G2 supernatant containing CD11b-Billiant Violet 605, anti-F4/80-AlexaFluor647 (clone CI:A3-1), anti-Ly-6G-APCCY7 (clone 1A8), anti-VCAM-1-Pacific Blue (clone 429), CD169-FITC (clone 3D6.112), Ter119-PECy7, biotinylated ER-HR3 antibody, and streptavidin-PE. Cell aggregates were gated as the tail of the forward scatter pulse width to detect erythroid islands [21].

In all stains, 5µg/mL 7-amino actinomycin D was added 15 minutes prior to acquisition to exclude dead leukocytes. Data were acquired on a CyAn (Dako Cytomation) flow cytometer and analyzed following compensation with single color controls using FloJo software (Tree Star, Ashland, OR). For sorting, cells were sorted on a FACS Aria cell sorter (BD Biosciences).

All antibodies were purchased from Biolegend except ER-HR3 and CD169 antibodies which were purchased from AbD Serotec.

Immunohistochemistry

Spleens and hind limb bones were fixed in PBS with 4% paraformalhehyde for 4 hours and 24 hours at 4°C respectively. Following bone decalcification, tissues were embedded in paraffin and 4-5 µm sections cut and placed on SuperFrost Plus® slides (Menzel, Germany). Sections were deparaffinized and re-hydrated with xylene and graded ethanol and washed in Tris-buffered saline. After antigen retrieval with trypsin a section from each sample was stained with unconjugated rat anti-ER-HR3. This was then detected using a two-step procedure as pervious described[22]. Consecutive sections from each sample were stained with biotinylated rat anti-Ter119 without antigen retrieval. Primary antibody was detected with horseradish peroxidase conjugated streptavidin (Dako, Glostrup, Denmark) and diaminobenzidine (DAB) chromogen. Sections were counterstained with Hematoxylin.

Double staining was undertaken with the first stage replicating the procedure for anti-ER-HR3 single staining. Prior to DAB development, sections were incubated with anti-Ter119-biotinylated antibody which was subsequently detected using a Vectorstain ABC-alkaline phosphatase kit (Vector Laboratories, Burlingame, CA). ER-HR3 expression was detected by DAB chromogen development and Ter119 expression by liquid permanent red (Dako). Double stained sections were counterstained with methyl green.

Specificity of staining was confirmed by comparison to serial sections stained with isotype matched control antibody. All sections were examined using an Olympus BX-51 microscope with a DP-70 digital camera and DP controller imaging software (Olympus).

RNA extraction and qRT-PCR

BM and spleen leukocytes were sorted directly into 2mL of Trizol (Life Technologies). Sort was paused sorted every 10^5 cells to mix collection tubes containing Trizol phase and sorted cells in aqueous phase. Collection tubes were then stored at -80°C before extraction of RNA

following manufacturer's instructions. Reverse transcription was performed using iScript cDNA kit (Biorad) as per manufacturer's instructions. qRT-PCR was performed using Taqman Universal PCR master mix (ABI) for *Csf3r* gene expression and SYBR Green PCR Master Mix (ABI) for mouse β2-microglobulin. The protocol for the PCR consisted of one cycle of 50°C (2 mins), followed by 95°C (10 mins) followed by 50 cycles of 95°C (10 sec) and 60°C (60 secs). Results were normalized relative to β2-microglobulin mRNA. Primers were *Csf3r* Taqman Gene Expression Assay (Mm00432735_m1) (ABI) and for β2-mciroglobulin: Forward 5'–CTGGTCTTTCTGGTGCTTGTC-3'; reverse 5'–GTATGTTCGGCTTCCCATTC-3'.

Statistical analyses

All data are presented as average ± SD. Statistical differences were calculated with a Student's t-test.

Results

G-CSF treatment causes BM anemia

The first indication G-CSF treatment was interfering with erythropoiesis was a marked whitening of the BM flushed from C57BL/6 mice mobilized for 2 to 6 days with G-CSF compared to BM flushed from saline-treated control mice (Fig. 1A). To further examine this, we stained BM cells with 7-amino actinomycin D to exclude dead leukocytes, Hoechst33342 (Ho) to distinguish nucleated leukocytes and erythroblasts from enucleated reticulocytes and erythrocytes, and antibodies specific for the erythroid lineage marker Ter119 and transferrin receptor CD71 to separate maturational stages of erythroid differentiation[23, 24].

A 4 day G-CSF treatment, which mobilizes HSC into the blood, reduced the number of $Ter119^{+}CD71^{+}$ erythroblasts 15-fold, $Ter119^{+}CD71^{low}$ polychromatic erythroblasts 1.7-fold, $Ter119^{+}CD71^{-}Ho^{+}$ orthochromatic erythroblasts 1.4-fold, and $Ter119^{+}Ho^{-}$ reticulocytes 4.5-fold (Fig. 1B and C). In contrast to this marked reduction in erythroblasts and reticulocytes, the number of $Ter119^{low}CD71^{+}Ho^{+}$ pro-erythroblasts was increased 4.4-fold. To confirm these results, we also stained BM with CD45, Ter119 and CD44 antibodies. Pro-erythroblasts were gated as $CD45^{-}$ $Ter119^{low}$ $CD44^{bright}$. The different differentiation stages of erythroblasts, reticulocytes and erythrocytes were gated within the $CD45^{-}$ $Ter119^{+}$ population according to decreasing CD44 expression and forward scatter [25, 26]. This staining and gating strategy confirmed the marked reduction in all differentiation stages of erythroblasts,

reticulocytes and erythrocytes with accumulation of pro-erythroblasts (Supplementary Fig. 1). As a result of decreased medullary erythropoiesis, hemoglobin concentration in the blood slightly and significantly decreased from 135.3±3.1 g/L to 116.7±3.1 g/L at day 2 of G-CSF treatment, and normalized at day 4 of treatment (Fig. 1D). Overall, this suggests that G-CSF causes transient a blockage in the maturation of pro-erythroblasts to erythroblasts, with loss of erythroblasts and reticulocytes in the BM (Fig. 1B and 1C).

Loss of F4/80$^+$VCAM-1$^+$ER-HR3$^+$CD169$^+$Ly-6G$^+$ macrophages in G-CSF mobilized BM

We have previously reported that G-CSF treatment causes a loss of F4/80$^+$Ly-6G$^+$ macrophages and collapse of HSC niche function in the BM [16, 18]. Another group recently reported that selective depletion of CD169$^+$ macrophages had similar effects on HSC mobilization and disruption of HSC niche function [15]. In order to determine whether F4/80$^+$Ly-6G$^+$ macrophages or CD169$^+$ macrophages include erythroid island macrophages, we performed additional phenotyping of these BM leukocytes with the ER-HR3 antibody, which identifies macrophages in erythropoietic islands in the mouse BM in steady-state[5, 27, 28]. We also assessed VCAM-1, as the interaction between VCAM-1 expressed by macrophages and its receptor integrin α4β1 expressed by erythroblasts is essential to erythropoietic recovery following cytotoxic challenge [29, 30].

By flow cytometry, the majority of CD11b$^+$F4/80$^+$VCAM-1$^+$ BM macrophages stained positive for both CD169 and ER-HR3 antigens (Fig. 2A). These CD11b$^+$F4/80$^+$VCAM-1$^+$ER-HR3$^+$CD169$^+$ macrophages could be further subdivided into Ly-6G$^-$ and Ly-6G$^+$ subsets. Interestingly a 4 day treatment with G-CSF caused 50% reduction in F4/80$^+$VCAM-1$^+$ER-HR3$^+$CD169$^+$ macrophages. Within this population, F4/80$^+$VCAM-1$^+$ER-HR3$^+$CD169$^+$Ly-6G$^+$ macrophages were decreased 35-fold leaving very rare macrophages of the phenotype in the BM of G-CSF treated mice whereas the number of F4/80$^+$VCAM-1$^+$ER-HR3$^+$CD169$^+$Ly-6G$^-$ macrophages remained unchanged (Fig. 2B). Of note, CD11b$^+$F4/80$^-$Ly-6G$^+$ granulocytes were negative for VCAM-1, CD169 and ER-HR3 antigens (data not shown). Considering that CD169 [21], VCAM-1 [30] and ER-HR3 [5, 28] antigens are expressed by subsets of macrophages that are functionally important for erythropoiesis, our results provide a finer mapping of BM macrophage subsets and suggest that CD11b$^+$F4/80$^+$VCAM-1$^+$ER-HR3$^+$CD169$^+$Ly-6G$^+$ macrophages represent erythroid island macrophages. Secondly, mobilizing doses of G-CSF caused a targeted and efficient depletion of these erythroid island macrophages resulting in defective erythropoiesis.

To further document the phenotype of erythroid island macrophages, we harvested BM cells in IMDM containing Ca^{2+} and Mg^{2+} to preserve cell-cell adhesive interactions between macrophages and erythroid cells. By gating on events with larger forward scatter peak width (FSC-W), we could identify cell aggregates that were positive for both the erythroid marker Ter119 and myeloid marker CD11b as previously reported[21]. These $Ter119^+CD11b^+$ erythroid-myeloid cell aggregates were enriched in $F4/80^+VCAM\text{-}1^+ER\text{-}HR3^+CD169^+Ly\text{-}6G^+$ compared to total BM macrophages (compare Fig. 2C with Fig. 2A). Importantly, events representing single cells according to low FSC-W contained very few events double positive for Ter119 and CD11b (Supplementary Figure 2) compared to cell aggregates (Fig. 2C) showing that in the BM cell aggregates preferentially contain erythroid and myeloid cells. A 4 day treatment with G-CSF in vivo caused a 6-fold reduction in the number of in $F4/80^+VCAM\text{-}1^+ER\text{-}HR3^+CD169^+Ly\text{-}6G^+$ macrophages engaged in these erythroid-meyloid cell aggregates (Fig. 2C) from 21,300±11,300 to 3,700±1,200 per femur ($p=0.02$) in saline treated and G-CSF treated mice respectively. In G-CSF-mobilized BM, $F4/80^-Ly\text{-}6G^+$ granulocytes were the main myeloid cell type engaged in $Ter119^+CD11b^+$ cell aggregates.

Immunohistochemistry staining of consecutive sections on mouse BM in steady-state clearly showed clusters of $Ter119^+$ erythroblasts associated with a very reticulated $ER\text{-}HR3^+$ macrophage at the center (Fig. 2D). This was confirmed on dual staining of BM sections for Ter119 and ER-HR3 antigens clearly showing long reticulated $ER\text{-}EHR3^+$ macrophages at the center of clusters of $Ter119^+$ nucleated erythroblasts (Supplementary Figure 3). This is in situ confirmation that ER-HR3 antigen is expressed by erythroid island macrophage in the mouse BM.

In order to determine whether the effect of G-CSF on macrophages was directly mediated via the G-CSF receptor, we sorted from the BM of untreated mice $F4/80^+VCAM\text{-}1^+ER\text{-}HR3^+CD169^+Ly\text{-}6G^+$ macrophages, $F4/80^+VCAM\text{-}1^+ER\text{-}HR3^+CD169^+Ly\text{-}6G^-$ macrophages, $F4/80^-Ly\text{-}6G^+$ granulocytes as well as surface IgM^+B220^+ and surface IgM^-B220^+ B cells as negative controls and extracted RNA. Quantitative real-time RT-PCR showed that G-CSF receptor mRNA (*Csf3r*) was abundantly expressed by these macrophages, whereas it was absent in IgM^+ and IgM^- B cells (Fig. 2E). This result suggests that G-CSF may act directly on erythroid island macrophages as they express its cognate receptor.

G-CSF treatment does not arrest splenic erythropoiesis

In contrast to the BM, G-CSF treatment significantly increased pro-erythroblasts, all populations of erythroblasts and reticulocytes in the spleen (Fig. 3A-B), thereby explaining why the blood anemia is mild (Fig. 1 D) despite a profound blockage of medullar erythropoiesis. Spleens were dissociated in culture medium with Ca^{2+} and Mg^{2+} using a GentleMACS Dissociator to preserve splenic macrophage integrity. Flow cytometry of cell aggregates with large FSC-W values showed the presence of $Ter119^{+}CD11b^{+}$ erythroid islands (albeit at a lower frequency than in the BM) associated with $F4/80^{+}VCAM\text{-}1^{+}ER\text{-}HR3^{+}CD169^{+}Ly\text{-}6G^{+}$ macrophages (Fig. 3C). In sharp contrast to the BM, a 4 day treatment with G-CSF in vivo increased 3.5-fold the number of cell aggregates between $Ter119^{+}$ erythroid cells and $CD11b^{+}$ myeloid cells per spleen (88,600±32,700 in saline versus 307,700±155,800 in G-CSF treated mice, p = 0.03), and did not significantly alter the number per spleen of $F4/80^{+}VCAM\text{-}1^{+}ER\text{-}HR3^{+}CD169^{+}Ly\text{-}6G^{+}$ macrophages engaged in these cell aggregates (Fig. 3C) (18,300±9,600 in saline versus 21,300±6,100 in G-CSF treated mice, p=0.62). By immunohistochemistry of serial sections, erythroid islands were detected exclusively in the red pulp and more specifically is the sub-cortical region of the spleen. Erythroid islands contained an $ER\text{-}HR3^{+}$ macrophage at the center (Fig. 3D). qRT-PCR on sorted splenic macrophages showed that $F4/80^{+}VCAM\text{-}1^{+}ER\text{-}HR3^{+}CD169^{+}Ly\text{-}6G^{+}$ macrophages also expressed *Csf3r* mRNA (Fig. 3E).

Medullar erythropoiesis restarts after cessation of G-CSF

As G-CSF is administered daily for 5-6 days in human donors, and has been shown to induce a slight (5-10%) but significant reduction in peripheral red blood cells [31], we next measured the recovery of erythropoiesis following cessation of G-CSF treatment. In mouse BM, the number of erythroblasts did not recover before day 5-7 following cessation of a 4 day course of G-CSF administration (Fig. 4A). In respect to pro-erythroblasts, their excessive number sharply decreased, between 24 hours and day 3 following G-CSF cessation and remained approximately half of their normal number until day 7 after G-CSF cessation.

In respect to the spleen, erythropoiesis remained elevated and normalization was more protracted than in the BM with a slow decrease in pro-erythroblasts and erythroblast numbers during the 7 days following cessation of G-CSF (Fig. 4C). This may explain why the blood concentration on hemoglobin decreased only slightly after a 4 day course of G-CSF (Fig. 4 D).

In respect to BM macrophages, the number of $F4/80^{+}VCAM\text{-}1^{+}ER\text{-}HR3^{+}CD169^{+}Ly\text{-}6G^{+}$, which were sharply suppressed after 4 days G-CSF, recovered by approximately 50%

24 hours after cessation of G-CSF. However complete recovery to steady-state levels was delayed as their number was still significantly decreased 7 days after G-CSF cessation (Fig. 4B). This suggests that a portion of BM erythroid island macrophages are restored as early as 24 hours following G-CSF treatment, which may kick-start differentiation of pro-erythroblasts into erythroblasts and reticulocytes in the BM. However complete normalization requires more than 7 days after cessation of G-CSF.

Macrophage depletion with clodronate-loaded liposomes blocks erythropoiesis in both BM and spleen

To further test the hypothesis that F4/80^{+}VCAM-1^{+}ER-HR3^{+}CD169^{+}Ly-6G^{+} macrophages depleted by G-CSF treatment are erythroid island macrophages indispensable to erythroblast maturation, we injected mice with clodronate-loaded liposomes intravenously every other day and sampled tissues after 4 days of this treatment. These liposomes efficiently kill phagocytes in a variety of tissues such as the BM and spleen [20]. Clodronate liposomes reduced the number of F4/80^{+}VCAM-1^{+}ER-HR3^{+}CD169^{+} macrophages 28-fold, with almost complete disappearance of F4/80^{+}VCAM-1^{+}ER-HR3^{+}CD169^{+}Ly-6G^{+} macrophages (Fig. 5C and 5D). Clodronate liposomes did not indiscriminately ablate all F4/80^{+} macrophages in the BM as F4/80^{+} VCAM-1^{-} macrophages remained relatively insensitive to clodronate liposome treatment (Fig. 5C).

In respect to the erythroid linage, clodronate liposome treatment also decreased the red coloration of BM flushes (Fig. 1A) suggesting impaired medullar erythropoiesis. Indeed clodronate liposome administration reduced the number of Ter119^{+} CD71^{+} erythroblasts 4.8-fold, Ter119^{+} CD71^{low} polychromatic erythroblasts 9.4 fold, Ter119^{+} CD71^{-} Ho^{+} orthochromatic erythroblasts 2.5-fold and Ter119^{+} CD71^{-} Ho^{-} reticulocytes 3-fold (Fig. 5A and 5B). Similar to G-CSF treatment, Ter119^{low} CD71^{+} Kit^{-} Ho^{+} pro-erythroblasts were increased 3.6-fold by clodronate liposomes (Fig. 5A and 5B). This suggests that similar to G-CSF, clodronate liposome treatment blocks the pro-erythroblast maturation into erythroblasts by depleting F4/80^{+} VCAM-1^{+} ER-HR3^{+} CD169^{+} Ly-6G^{+} macrophages at the center of erythroid islands.

In sharp contrast to G-CSF treatment, clodronate liposomes caused an extended depletion of Ter119^{+} CD71^{+} erythroblasts and Ter119^{+} CD71^{low} polychromatic erythroblasts in the spleen whereas reticulocyte numbers were unaltered (Supplementary Figure 4). Therefore, unlike G-CSF, non-selective depletion of phagocytes by clodronate liposomes impairs erythropoiesis in both BM and spleen.

Selective depletion of CD169$^+$ macrophages blocks erythropoiesis in both BM and Spleen

Finally, to further document the role of CD169$^+$ macrophages in erythropoiesis, we used *Siglec1*$^{DTR/+}$ mice with a simian diphtheria toxin receptor (DTR) knocked in the mouse *Siglec1* gene that encodes the CD169 antigen. Diphtheria toxin (DPT) binds poorly to mouse cells however the simian DTR has a high affinity for DPT. As such, low doses of DPT (10 to 25 µg/kg) selectively kill CD169$^+$ macrophages which express simian DTR in *Siglec1*$^{DTR/+}$ mice [19]. As DPT may cause an immune reaction by itself, we compared the effect of DPT versus saline in wild-type (*Siglec1*$^{+/+}$) and *Siglec1*$^{DTR/+}$ mice.

Of note, a 4 day course of DPT caused a slight but measurable down-regulation of CD169 expression on macrophages in wild-type mice but not any of the other antigens investigated herein (Fig. 6A). Likewise *Siglec1*$^{DTR/+}$ mice treated with saline had reduced CD169 expression compared to saline-treated wild-type due to the loss of one of the two alleles of the *Siglec1* gene (Fig. 6A-B).

A 4 day course of 10µg/kg DPT markedly reduced the frequency and number of F4/80$^+$ macrophages expressing VCAM-1 (Fig. 6A) in *Siglec1*$^{DTR/+}$ mice resulting in a 26.8-fold reduction in the number of F4/80$^+$VCAM-1$^+$ER-HR3$^+$CD169$^+$Ly-6G$^+$ macrophages compared to *Siglec1*$^{DTR/+}$ mice treated with saline (Fig. 6A-B).

Similar to G-CSF and clodronate liposomes in wild-type mice, DPT treatment in *Siglec1*$^{DTR/+}$ mice reduced the red coloration of flushed BM whereas DPT had a mild effect on the red coloration of the BM from *Siglec1*$^{+/+}$ wild-type C57BL/6 mice (Supplementary Fig. 5). As recently reported [21], after DPT treatment the numbers of Ter119$^+$CD71^{bright} erythroblasts, Ter119$^+$CD71$^+$ polychromatic erythroblasts and Ter119$^+$CD71$^-$ reticulocytes in BM (Supplementary Figure 5) were significantly reduced in the BM, with accumulation of pro-erythroblasts. However, in sharp contrast to the previous two models, depletion of CD169$^+$ macrophages had only a marginal effect on the number of BM reticulocytes.

Finally, similar to non-selective phagocyte depletion with clodronate liposomes, selective depletion of CD169$^+$ macrophages impaired splenic erythropoiesis with significant reduction in the numbers of erythroblasts and polychromatic erythroblasts (Supplementary Figure 6).

Discussion

Amongst differentiated cells of the body, macrophages are the most functionally plastic [32, 33]. They can fulfill a large number of functions in innate immunity (e.g. phagocytosis of pathogens and dead cells), regulation of adaptive immunity [34], tissue development, maintenance and repair[35, 36]. Macrophages also play an essential role in pathogenesis caused by excessive inflammatory responses, and in various stages of cancer development [37, 38] such as the initial smoldering inflammation leading to malignant transformation, tumor-associated neo-angiogenesis [39], metastasis [40, 41], immune suppression [42] and response to treatment [43]. Although macrophage populations and function have been extensively studied in these solid tissues, paradoxically relatively little is known of macrophage populations and function in the BM.

We and others have recently reported that specific subsets of BM macrophages are critical to the maintenance of osteoblasts and bone formation at the endosteum [16, 22], and of HSC niches in the mouse [16]. Indeed depletion of macrophages stops bone formation and induces HSC mobilization into the blood [16]. A subset of BM macrophages has also been known for a long time to participate to erythropoiesis as suggested by the location of a central macrophage in erythroid islands in mouse BM, spleen and liver [2, 3, 28]. As G-CSF triggers HSC mobilization by impairing the function of HSC niche-supportive macrophages in the BM [16, 17], we explored the effect of G-CSF on erythropoiesis in the mouse. G-CSF caused the loss of BM macrophages expressing VCAM-1, CD169 and ER-HR3 antigen, all of which have been shown to be important to erythropoiesis in the BM, spleen or liver [5, 21, 28, 30]. G-CSF caused a concomitant blockage of medullar erythropoiesis with accumulation of pro-erythroblasts and sharp reduction in the numbers of maturing erythroblasts and reticulocytes suggesting a blockade in pro-erythroblast maturation and defective erythroblast maturation. This effect was unique to the BM as splenic erythropoiesis was not inhibited but increased by G-CSF treatment. As 1) G-CSF treatment caused a 35-fold reduction in the number of $CD11b^{+}F4/80^{+}VCAM\text{-}1^{+}ER\text{-}HR3^{+}CD169^{+}Ly\text{-}6G^{+}$ BM macrophages, 2) this macrophage phenotype was specifically enriched in BM cell aggregates containing both myeloid and erythroid cells, and 3) erythroid island macrophages expressed ER-HR3 antigen on BM sections, we propose that $CD11b^{+}F4/80^{+}VCAM\text{-}1^{+}ER\text{-}HR3^{+}CD169^{+}Ly\text{-}6G^{+}$ macrophages represent erythroid island macrophages that are necessary to erythroblast maturation into reticulocytes, and that G-CSF treatment depletes these macrophages causing a blockade in medullar erythropoiesis. This conclusion is further substantiated by our observation that treatment of wild-type mice with clodronate-loaded liposomes, or treatment of *Siglec1*$^{DTR/+}$ mice with DPT also caused similar loss of $F4/80^{+}VCAM\text{-}1^{+}ER\text{-}HR3^{+}CD169^{+}Ly\text{-}6G^{+}$

macrophages and blockade of erythropoiesis. Our results are consistent with previous observations that ER-HR3$^+$ macrophages are highly phagocytic in vivo [27, 44] and should therefore be depleted by clodronate-loaded liposomes.

Erythroid island macrophages have been proposed to facilitate Fe^{2+} transport into erythroblasts and actively participate to their enucleation during the final stages of erythroblast maturation. Our results with G-CSF and clodronate-loaded liposomes and in *Siglec1*^{DTR} mice clearly indicate that in addition to these roles, erythroid island macrophages are necessary to the maturation of pro-erythroblasts to erythroblasts. Whether this is linked to the inability of erythroblasts to survive in the absence of macrophage-mediated iron import or to secrete supportive cytokines remains to be determined.

Our results are also consistent with a recent report showing that erythropoietic island macrophages isolated from the mouse BM are CD169$^+$ and that their depletion results in a blockade of medullar erythropoiesis [21]. Our data identifies more precisely the phenotype of these erythroblast-supportive macrophages as CD11b$^+$ F4/80$^+$ VCAM-1$^+$ ER-HR3$^+$ CD169$^+$ Ly-6G$^+$. Of note, G-CSF and clodronate liposome treatments significantly increased the number of CD11b$^+$ F4/80$^-$ Ly-6G$^+$ granulocytes (data not shown), consistent with our previous observations [16, 18]. Therefore, the Ly-6G antigen is not exclusively specific of granulocytes as it is also expressed by a subset of macrophages that support erythroblasts (herein) and HSCs [16] in the BM.

Whist others have studied these erythropoietic island macrophages using only one or two antigens, we have examined the expression of a number of antigens at once, allowing for a more precise identification of the erythropoietic island macrophages. This will enable further studies on these macrophages in steady-state as well as in disease states. Anemia is one of the first symptoms associated with a number of hematological malignancies, including chronic and acute myeloid leukemia, and myelodysplastic syndrome. The possibility that erythropoietic island macrophages may be involved or perturbed in the initial stages of these diseases has not been investigated because of the lack of precise markers for these macrophages.

In respect to the function of these macrophage antigens in regulating erythropoiesis, we noticed that *Siglec1*$^{DTR/DTR}$ mice, which are functionally knocked-out for the *Siglec1* gene and CD169 expression, have normal numbers of pro-erythroblasts, erythroblasts and reticulocytes in their BM (data not shown). Therefore the CD169 antigen, whilst useful to identify or target erythroblast supportive macrophages, is functionally dispensable for erythroblast maturation. We confirmed that the ER-HR3 antigen, which identifies erythroid islands in spleen and liver

[5, 27, 28], also identifies erythroid island macrophages in the BM. However, the exact identity of this antigen and whether its expression is necessary to support erythropoiesis remain unknown [44]. On the other hand, it is well established that within the BM hematopoietic compartment, VCAM-1 is mainly expressed by macrophages[30], and mediates adhesion of erythroblasts to erythroid island macrophages via integrin α4β1 expressed by erythroblasts [45, 46]. Furthermore conditional deletion of the *Vcam1* or *Itga4* gene in mice impairs erythropoietic recovery following cytotoxic or phenylhydrazine challenge [29, 30], whereas administration of function-blocking anti-VCAM-1 antibody impairs erythropoietic recovery following BM transplantation [21].

Although the BM is the main site of erythropoiesis in adults in steady-state, the spleen and liver can become important extramedullary erythropoietic organs when the BM is compromised as observed in some hematological neoplasms [28, 47]. Mobilizing treatment with G-CSF, while blocking medullar erythropoiesis, significantly increased splenic erythropoiesis. In contrast, both non-selective depletion of phagocytes with clodronate liposomes and selective ablation of $CD169^+$ macrophages in the *Siglec1*$^{DTR/+}$ models blocked splenic as well as medullar erythropoiesis probably because in both these models, macrophages are depleted regardless of their anatomical location. Interestingly however, Chow et al have recently suggested that despite blockade of both medullar and splenic erythropoiesis in the *Siglec1*$^{DTR/+}$ model, mice did not become anemic as a result of a lengthening of erythrocyte turn-over following $CD169^+$ macrophage depletion in the spleen [21]. Such a mechanism is unlikely to be at play in G-CSF-mobilized mice as G-CSF does not deplete splenic macrophages.

It remains unclear how G-CSF causes the loss of $CD11b^+F4/80^+VCAM\text{-}1^+ER\text{-}HR3^+$ $CD169^+Ly\text{-}6G^+$ macrophages in the BM without altering their number in the spleen, as these cells express the receptor *Csf3r* mRNA in both tissues. In the absence of monoclonal antibody specific for mouse G-CSF receptor, we could not confirm these results at the protein level. It therefore remains possible that the expression of the receptor at the cell surface or signaling upon G-CSF binding is context dependent and different in each tissue.

In respect to the relevance of our results to humans, the effect of G-CSF on human erythropoiesis has not been extensively studied. However a similar effect may occur as Juarez et al recently reported that the number of red blood cells also decreased following G-CSF induced mobilization by approximately 5-10% in both in allogeneic (from 4.9±0.4 to 4.7±0.5 x 10^9/mL, p=10^{-4}) and autologous (from 3.9±0.6 to 3.4±0.4 x 10^9/mL, p=0.002) settings [31] despite the fact that human red blood cells have a 4 times longer half-life than mouse red

blood cells (50-55 days [48] versus 14 days [49]). Although this remains to be confirmed experimentally on BM samples from mobilized patients, G-CSF may also cause a transient arrest in medullar erythropoiesis in humans by interfering with BM macrophages that support erythropoiesis, with possible compensation in the spleen.

In conclusion, G-CSF doses used to mobilize HSCs in transplantation donors transiently impair the function of different subsets of tissue supportive macrophages in the mouse BM particularly osteomacs that support bone forming osteoblasts [22, 50], HSC niche-supportive macrophages [15-17] and erythropoietic island macrophages (herein). This further demonstrates that macrophages are potent relays of innate immunity and inflammation on i) osteogenic, ii) hematopoietic and iii) erythropoietic processes in the BM and that treatments or agents that affect these macrophages, are likely to affect these three processes concomitantly [12].

Acknowledgements

We thank Dr Andrew Perkins for helpful discussions throughout this work and Dalia Khalil for cell sorting. This work was supported by Project Grant 1046590 from the National Health and Medical Research Council of Australia (to JPL, ARP and IGW) and additional support from the Mater Foundation. RNJ was supported by an Australian Post-graduate Award from the Commonwealth of Australia, JPL and IGW are supported by a Senior Research Fellowship #1044091 and a Career Development Fellowship (#1033736) respectively from the National Health and Medical Research Council.

Conflict of interest

The authors have no conflict of interest to declare.

References

[1] Bessis M. L'ilot erythroblastique. Unite fonctionelle de la moelle osseuse. Rev Hematol. 1958;13:8-11.
[2] Bessis MC, Breton-Gorius J. Iron Metabolism in the Bone Marrow as Seen by Electron Microscopy: A Critical Review. Blood. 1962;19:635-663.
[3] Mohandas N, Prenant M. Three-dimensional model of bone marrow. Blood. 1978;51:633-643.
[4] Chasis JA, Mohandas N. Erythroblastic islands: niches for erythropoiesis. Blood. 2008;112:470-478.
[5] Sonoda Y, Sasaki K. Surface morphology of the central macrophages of erythroblastic islets in the spleen of aged and pregnant mice: an immunohistochemical light microscopic study. Archives of Histology and Cytology. 2008;71:155-161.
[6] Leimberg MJ, Prus E, Konijn AM, Fibach E. Macrophages function as a ferritin iron source for cultured human erythroid precursors. Journal of Cellular Biochemistry. 2008;103:1211-1218.
[7] Sawada K, Krantz SB, Dessypris EN, Koury ST, Sawyer ST. Human colony-forming units-erythroid do not require accessory cells, but do require direct interaction with insulin-like growth factor I and/or insulin for erythroid development. The Journal of Clinical Investigation. 1989;83:1701-1709.
[8] Manwani D, Bieker JJ. The Erythroblastic Island. In: James JB, ed. Current Topics in Developmental Biology: Academic Press; 2008. p. 23-53.
[9] Skutelsky E, Danon D. On the expulsion of the erythroid nucleus and its phagocytosis. The Anatomical Record. 1972;173:123-126.
[10] Soni S, Bala S, Gwynn B, Sahr KE, Peters LL, Hanspal M. Absence of erythroblast macrophage protein (Emp) leads to failure of erythroblast nuclear extrusion. Journal of Biological Chemistry. 2006;281:20181-20189.
[11] Levesque JP, Helwani FM, Winkler IG. The endosteal 'osteoblastic' niche and its role in hematopoietic stem cell homing and mobilization. Leukemia. 2010;24:1979-1992.
[12] Winkler IG, Levesque JP. Mechanisms of hematopoietic stem cell mobilization: When innate immunity assails the cells that make blood and bone. Exp Hematol. 2006;34:996-1009.
[13] Levesque JP, Hendy J, Takamatsu Y, Simmons PJ, Bendall LJ. Disruption of the CXCR4/CXCL12 chemotactic interaction during hematopoietic stem cell mobilization induced by GCSF or cyclophosphamide. J Clin Invest. 2003;111:187-196.
[14] Levesque JP, Takamatsu Y, Nilsson SK, Haylock DN, Simmons PJ. Vascular cell adhesion molecule-1 (CD106) is cleaved by neutrophil proteases in the bone marrow following hematopoietic progenitor cell mobilization by granulocyte colony-stimulating factor. Blood. 2001;98:1289-1297.
[15] Chow A, Lucas D, Hidalgo A, et al. Bone marrow CD169+ macrophages promote the retention of hematopoietic stem and progenitor cells in the mesenchymal stem cell niche. The Journal of Experimental Medicine. 2011;208:261-271.
[16] Winkler IG, Sims NA, Pettit AR, et al. Bone marrow macrophages maintain hematopoietic stem cell (HSC) niches and their depletion mobilizes HSCs. Blood. 2010;116:4815-4828.
[17] Christopher MJ, Rao M, Liu F, Woloszynek JR, Link DC. Expression of the G-CSF receptor in monocytic cells is sufficient to mediate hematopoietic progenitor mobilization by G-CSF in mice. The Journal of Experimental Medicine. 2011;208:251-260.
[18] Winkler IG, Pettit AR, Raggatt LJ, et al. Hematopoietic stem cell mobilizing agents G-CSF, cyclophosphamide or AMD3100 have distinct mechanisms of action on bone marrow HSC niches and bone formation. Leukemia. 2012;26:1594-1601.

[19] Miyake Y, Asano K, Kaise H, Uemura M, Nakayama M, Tanaka M. Critical role of macrophages in the marginal zone in the suppression of immune responses to apoptotic cell–associated antigens. The Journal of Clinical Investigation. 2007;117:2268-2278.
[20] van Rooijen N, Hendrikx E. Liposomes for specific depletion of macrophages from organs and tissues. Methods Mol Biol. 2010;605:189-203.
[21] Chow A, Huggins M, Ahmed J, et al. CD169+ macrophages provide a niche promoting erythropoiesis under homeostasis and stress. Nat Med. 2013;19:429-436.
[22] Chang MK, Raggatt L-J, Alexander KA, et al. Osteal tissue macrophages are intercalated throughout human and mouse bone lining tissues and regulate osteoblast function in vitro and in vivo. J Immunol. 2008;181:1232-1244.
[23] Zhang J, Socolovsky M, Gross AW, Lodish HF. Role of Ras signaling in erythroid differentiation of mouse fetal liver cells: functional analysis by a flow cytometry–based novel culture system. Blood. 2003;102:3938-3946.
[24] Kingsley PD, Greenfest-Allen E, Frame JM, et al. Ontogeny of erythroid gene expression. Blood. 2013;121:e5-e13.
[25] Chen K, Liu J, Heck S, Chasis JA, An X, Mohandas N. Resolving the distinct stages in erythroid differentiation based on dynamic changes in membrane protein expression during erythropoiesis. Proceedings of the National Academy of Sciences. 2009;106:17413-17418.
[26] Liu J, Zhang J, Ginzburg Y, et al. Quantitative analysis of murine terminal erythroid differentiation in vivo: novel method to study normal and disordered erythropoiesis. Blood. 2013;121:e43-e49.
[27] de Jong JP, Voerman JS, van der Sluijs-Gelling AJ, Willemsen R, Ploemacher RE. A monoclonal antibody (ER-HR3) against murine macrophages. I. Ontogeny, distribution and enzyme histochemical characterization of ER-HR3-positive cells. Cell Tissue Res. 1994;275:567-576.
[28] Sonoda Y, Sasaki K. Hepatic Extramedullary Hematopoiesis and Macrophages in the Adult Mouse: Histometrical and Immunohistochemical Studies. Cells Tissues Organs. 2012;196:555-564.
[29] Scott LM, Priestley GV, Papayannopoulou T. Deletion of {alpha}4 Integrins from Adult Hematopoietic Cells Reveals Roles in Homeostasis, Regeneration, and Homing. Mol Cell Biol. 2003;23:9349-9360.
[30] Ulyanova T, Scott LM, Priestley GV, et al. VCAM-1 expression in adult hematopoietic and nonhematopoietic cells is controlled by tissue-inductive signals and reflects their developmental origin. Blood. 2005;106:86-94.
[31] Juarez JG, Harun N, Thien M, et al. Sphingosine-1-phosphate facilitates trafficking of hematopoietic stem cells and their mobilization by CXCR4 antagonists in mice. Blood. 2012;119:707-716.
[32] Pollard JW. Trophic macrophages in development and disease. Nat Rev Immunol. 2009;9:259-270.
[33] Sica A, Mantovani A. Macrophage plasticity and polarization: in vivo veritas. J Clin Invest. 2012;122:787-795.
[34] Galli SJ, Borregaard N, Wynn TA. Phenotypic and functional plasticity of cells of innate immunity: macrophages, mast cells and neutrophils. Nat Immunol. 2011;12:1035-1044.
[35] Mantovani A, Biswas SK, Galdiero MR, Sica A, Locati M. Macrophage plasticity and polarization in tissue repair and remodelling. J Pathol. 2013;229:176-185.
[36] Willenborg S, Lucas T, van Loo G, et al. CCR2 recruits an inflammatory macrophage subpopulation critical for angiogenesis in tissue repair. Blood. 2012;120:613-625.
[37] Mantovani A. MSCs, macrophages, and cancer: A dangerous ménage-à-trois. Cell Stem Cell. 2012;11:730-732.
[38] Mantovani A, Sica A. Macrophages, innate immunity and cancer: balance, tolerance and diversity. Curr Opin Immunol. 2010;22:231-237.

[39] Mazzieri R, Pucci F, Moi D, et al. Targeting the ANG2/TIE2 axis inhibits tumor growth and metastasis by impairing angiogenesis and disabling rebounds of proangiogenic myeloid cells. Cancer Cell. 2011;19:512-526.
[40] Qian BZ, Li J, Zhang H, et al. CCL2 recruits inflammatory monocytes to facilitate breast-tumour metastasis. Nature. 2011;472:222-227.
[41] Qian BZ, Pollard JW. Macrophage diversity enhances tumor progression and metastasis. Cell. 2010;141:39-51.
[42] Gabrilovich DI, Nagaraj S. Myeloid-derived suppressor cells as regulators of the immune system. Nat Rev Immunol. 2009;9:162-174.
[43] Jinushi M, Chiba S, Yoshiyama H, et al. Tumor-associated macrophages regulate tumorigenicity and anticancer drug responses of cancer stem/initiating cells. Proc Natl Acad Sci USA. 2011;108:12425-12430.
[44] de Jong JP, Leenen PJ, Voerman JS, van der Sluijs-Gelling AJ, Ploemacher RE. A monoclonal antibody (ER-HR3) against murine macrophages. II. Biochemical and functional aspects of the ER-HR3 antigen. Cell Tissue Res. 1994;275:577-585.
[45] Rosemblatt M, Vuillet-Gaugler MH, Leroy C, Coulombel L. Coexpression of two fibronectin receptors, VLA-4 and VLA-5, by immature human erythroblastic precursor cells. The Journal of Clinical Investigation. 1991;87:6-11.
[46] Sadahira Y, Yoshino T, Monobe Y. Very late activation antigen 4-vascular cell adhesion molecule 1 interaction is involved in the formation of erythroblastic islands. The Journal of Experimental Medicine. 1995;181:411-415.
[47] Prakash S, Hoffman R, Barouk S, Wang YL, Knowles DM, Orazi A. Splenic extramedullary hematopoietic proliferation in Philadelphia chromosome-negative myeloproliferative neoplasms: heterogeneous morphology and cytological composition. Mod Pathol. 2012;25:815-827.
[48] Mock DM, Lankford GL, Widness JA, Burmeister LF, Kahn D, Strauss RG. Measurement of red cell survival using biotin-labeled red cells: validation against 51Cr-labeled red cells. Transfusion. 1999;39:156-162.
[49] Gardenghi S, Renaud TM, Meloni A, et al. Distinct roles for hepcidin and interleukin-6 in the recovery from anemia in mice injected with heat-killed Brucella abortus. Blood. 2014;123:1137-1145.
[50] Takamatsu Y, Simmons PJ, Moore RJ, Morris HA, To LB, Levesque JP. Osteoclast-mediated bone resorption is stimulated during short-term administration of granulocyte colony-stimulating factor but is not responsible for hematopoietic progenitor cell mobilization. Blood. 1998;92:3465-3473.

Figure legends

Figure 1. G-CSF blocks medullary erythropoiesis. (A) Photograph of mouse femoral BM flushed into 1 mL PBS after 4 day treatment with saline, G-CSF or clodronate loaded liposomes. Note the loss of red coloration in mice treated with G-CSF or clodronate-loaded liposomes. (B) Representative flow cytometry dot-plots of mouse BM after a 4 day treatment with G-CSF or saline. The left dot-plots show Ter119 versus CD71 amongst Ho^+ nucleated cells. Pro-erythroblasts were gated as $Ter119^{low}CD71^+$ (population I), erythroblasts as $Ter119^+CD71^+$ (population II), polychromatic erythroblasts as $Ter119^+CD71^{low}$ (population III), and orthochromatic erythroblasts as $Ter119^+CD71^{low}$ (population IV). In the right dot-plots, reticulocytes are gated as $Ter119^+$ Ho^- $Ter119^+CD71^{low}$ (population V). (C) Quantification of erythroid populations in the femoral BM after a 4 day G-CSF (G) or saline (Sal) treatment. (D) Hemoglobin concentration in the blood of mice treated with saline (Sal), G-CSF for 2 days (G2), or G-CSF for 4 days (G4). Data are mean ± SD of 4 mice per group from one representative experiment among 6 independent repeats. Differences were evaluated with a t-test (* $p \leq 0.05$; ** $p \leq 0.01$; *** $p \leq 0.001$).

Figure 2. G-CSF treatment reduces the number of $F4/80^+$ $VCAM1^+$ $CD169^+$ $ER\text{-}HR3^+$ $Ly6\text{-}G^+$ erythroid island macrophages in the BM. (A) Representative flow cytometry dot-plots of mouse BM after a 4 day treatment with G-CSF or saline. BM $F4/80^+$ macrophages were gated from $CD11b^+$ myeloid cells and further subgated from expression of VCAM-1, CD169, ER-HR3 and Ly6-G antigens (B) Quantification of macrophage populations in femoral BM after a 4 day G-CSF (G) or saline (Sal) treatment. Data are mean ± SD of 4 mice per group from one representative experiment among 4 independent repeats. Differences were evaluated with a t-test (* $p \leq 0.05$; ** $p \leq 0.01$; *** $p \leq 0.001$). (C) Representative phenotype of BM cell aggregates (with high forward scatter peak width) containing $Ter119^+$ erythroid cells and $CD11b^+$ myeloid cells in mice treated for 4 days with saline or with G-CSF. Note that the myeloid cells contained in these aggregates are very enriched in $F4/80^+$ $VCAM1^+$ $CD169^+$ $ER\text{-}HR3^+$ $Ly6\text{-}G^+$ macrophages compared to whole BM in panel A (2 independent experiments, n=4 per experiment). (D) Double immunohistochemistry for ER-HR3 (brown) and Ter119 (red) antigens in femoral BM from from mice treated with saline. Reticulated $ER\text{-}HR3^+$ macrophages are indicated by arrows at the center of $Ter119^+$ (arrow heads)

erythroid islands. (E) Quantification of *Csf3r* mRNA by qRT-PCR on F4/80$^-$ Ly6-G$^+$ granulocytes, F4/80$^+$ VCAM1$^+$ CD169$^+$ ER-HR3$^+$ Ly6-G$^+$ macrophages and F4/80$^+$ VCAM1$^+$ CD169$^+$ ER-HR3$^+$ Ly6-G$^-$ macrophages sorted from the BM of saline treated mice. Sorted sIgM$^-$ and sIgM$^+$ B cells were used as negative controls. Data are standardized to results from F4/80$^-$ Ly6-G$^+$ granulocytes and are mean ± SD of 4 mice (4 independent sorts) per phenotype. *Csf3r* mRNA was undetectable in B cells.

Figure 3. G-CSF treatment does not inhibit erythropoiesis in the spleen. (A) Representative flow cytometry dot-plots of mouse spleens after a 4 day treatment with G-CSF or saline. The left panels show Ter119 versus CD71 amongst Ho$^+$ nucleated cells (Pro-erythroblasts were gated as Ter119^{low}CD71$^+$, erythroblasts as Ter119$^+$CD71$^+$, polychromatic erythroblasts as Ter119$^+$CD71^{low}).In the right panel reticulocytes are gated as Ter119$^+$ Ho$^-$. (B) Quantification of erythroid populations in spleens after a 4 day G-CSF (G) or saline (Sal) treatment. Data are mean ± SD of 4 mice per group from one representative experiment among 4 independent repeats. Differences were evaluated with a t-test (* $p \leq 0.05$; ** $p \leq 0.01$; *** $p \leq 0.001$). (C) Representative phenotype of splenic cell aggregates (with high forward scatter peak width) containing Ter119$^+$ erythroid cells and CD11b$^+$ myeloid cells in mice treated for 4 days with saline or G-CSF. (D) Immunohistochemistry of ER-HR3 and Ter119 on consecutive sections of spleens from mice treated with saline. Yellow arrow in top panel shows reticulated ER-HR3$^+$ macrophage at the center of Ter119$^+$ erythroid islands indicated by green arrows in bottom panel. Note that erythroid islands were enriched in the cortical are in the red pulp. (E) Quantification of *Csf3r* mRNA by qRT-PCR on F4/80$^-$ Ly6-G$^+$ granulocytes, F4/80$^+$ VCAM1$^+$ CD169$^+$ ER-HR3$^+$ Ly6-G$^+$ macrophages and F4/80$^+$ VCAM1$^+$ CD169$^+$ ER-HR3$^+$ Ly6-G$^-$ macrophages sorted from the spleens of saline treated mice. Sorted sIgM$^-$ and sIgM$^+$ B cells were used as negative controls. Data are standardized to results from F4/80$^-$ Ly6-G$^+$ granulocytes and are mean ± SD of 4 mice (4 independent sorts) per phenotype. *Csf3r* mRNA was undetectable in B cells.

Figure 4. Kinetics of erythropoietic recovery in the BM following cessation of G-CSF. Mice were treated for 4 days with G-CSF and the numbers of erythroid cells (A), and macrophages (B) was quantified in the femoral BM by flow cytometry at the indicated time-points after cessation of G-CSF. (C) Kinetics of erythroid cell numbers in the spleen after cessation of G-CSF treatment. (D) Kinetics of blood hemoglobin concentration after cessation of G-CSF treatment. Day 0 represents the last day of G-CSF. S on the abscissa indicates the values

obtained from control mice treated for 4 days with saline instead of G-CSF. Data are mean ± SD of 4 mice per group. Differences were evaluated with a t-test (* $p \leq 0.05$; ** $p \leq 0.01$; *** $p \leq 0.001$).

Figure 5. Macrophage depletion with clodronate-loaded liposomes stops medullary eythropoiesis. (A) Representative flow cytometry dot-plots of mouse BM after a 3 day treatment with clodronate-loaded liposomes or saline. The left panels show Ter119 versus CD71 amongst Ho^+ nucleated cells (Pro-erythroblasts were gated as $Ter119^{low}CD71^+$, erythroblasts as $Ter119^+CD71^+$, polychromatic erythroblasts as $Ter119^+CD71^{low}$). In the right panel reticulocytes are gated as $Ter119^+$ Ho^-. (B) Quantification of erythroid populations in the femoral BM after a 3 day clodronate liposome (Clo) or saline (Sal) treatment. (C) Representative flow cytometry dot-plots of mouse BM after a 3 day treatment with clodronate-loaded liposomes or PBS-loaded liposomes. BM $F4/80^+$ macrophages were gated from $CD11b^+$ myeloid cells and further subgated from expression of VCAM-1, CD169, ER-HR3 and Ly6-G antigens (B) Quantification of macrophage populations in femoral BM after a 3 day clodronate loaded liposmes (Clo) or saline (Sal) treatment. Data are mean ± SD of 4 mice per group from one representative experiment out of 2 independent repeats. Differences were evaluated with a t-test (* $p \leq 0.05$; ** $p \leq 0.01$; *** $p \leq 0.001$).

Figure 6. Depletion of $CD169^+$ macrophages induces loss of erythroid island macrophages in the BM. Representative flow cytometry dot-plots of mouse BM after a 4 day treatment with saline or DPT in wild-type mice or *Siglec1*$^{DTR/+}$ mice. (A) Typical flow cytometry dot-plots showing BM $F4/80^+$ macrophages gated from $CD11b^+$ myeloid cells and further subgated from expression of VCAM-1, CD169, ER-HR3 and Ly6-G antigens (B) Quantification of macrophage populations in femoral BM after a 4 day treatment with saline or DPT in wild-type mice or $Siglec1^{DTR/+}$ mice. DTR indicates the presence (+) or absence (-) of the *Siglec1*^{DTR} mutant allele. DPT indicates treatment with DPT (+) or saline (-). Data are mean ± SD of 3-5 mice per group from one representative experiment out of 2 independent repeats. Differences were evaluated with a t-test (* $p \leq 0.05$; ** $p \leq 0.01$; *** $p \leq 0.001$).

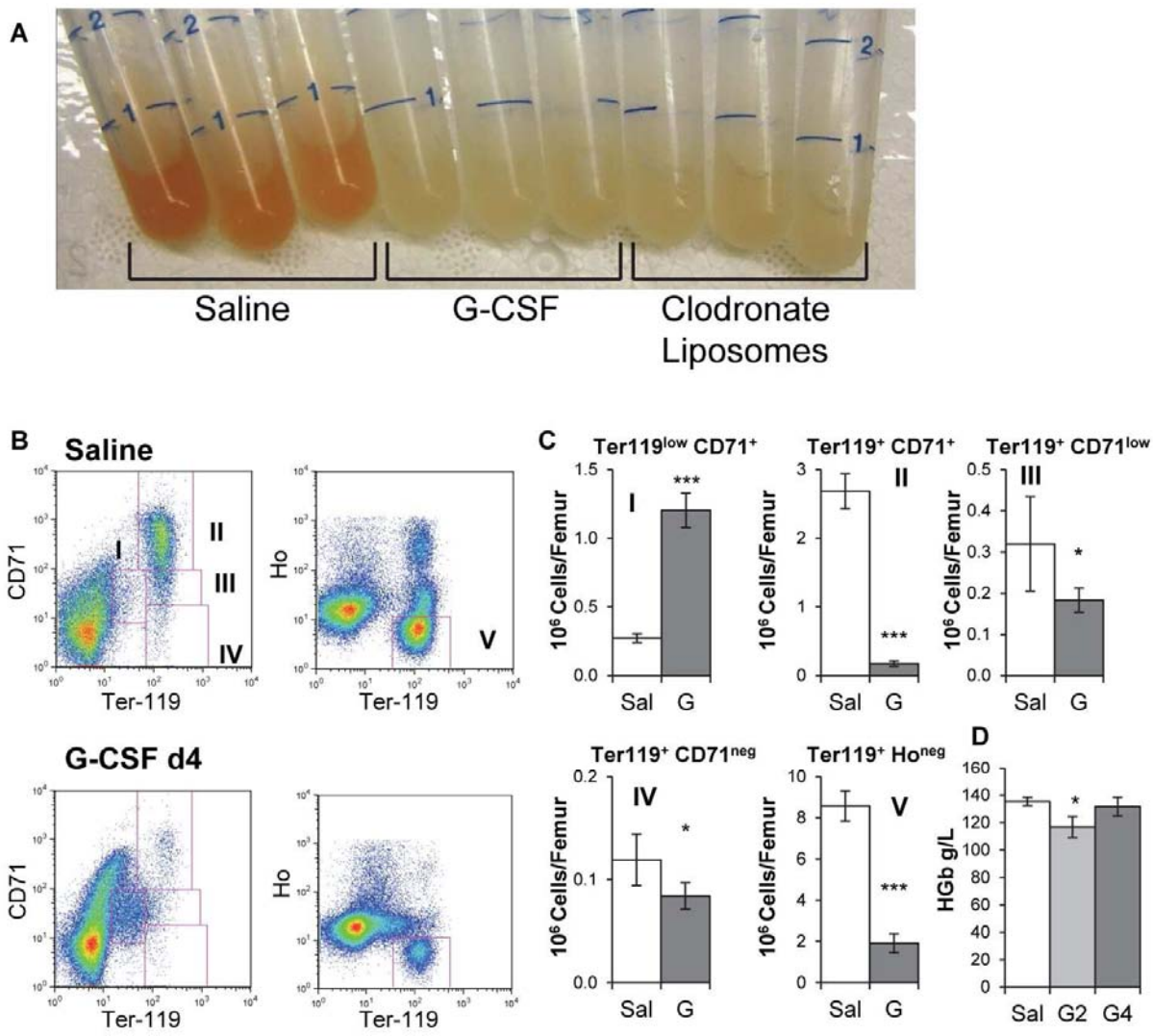

Figure 1

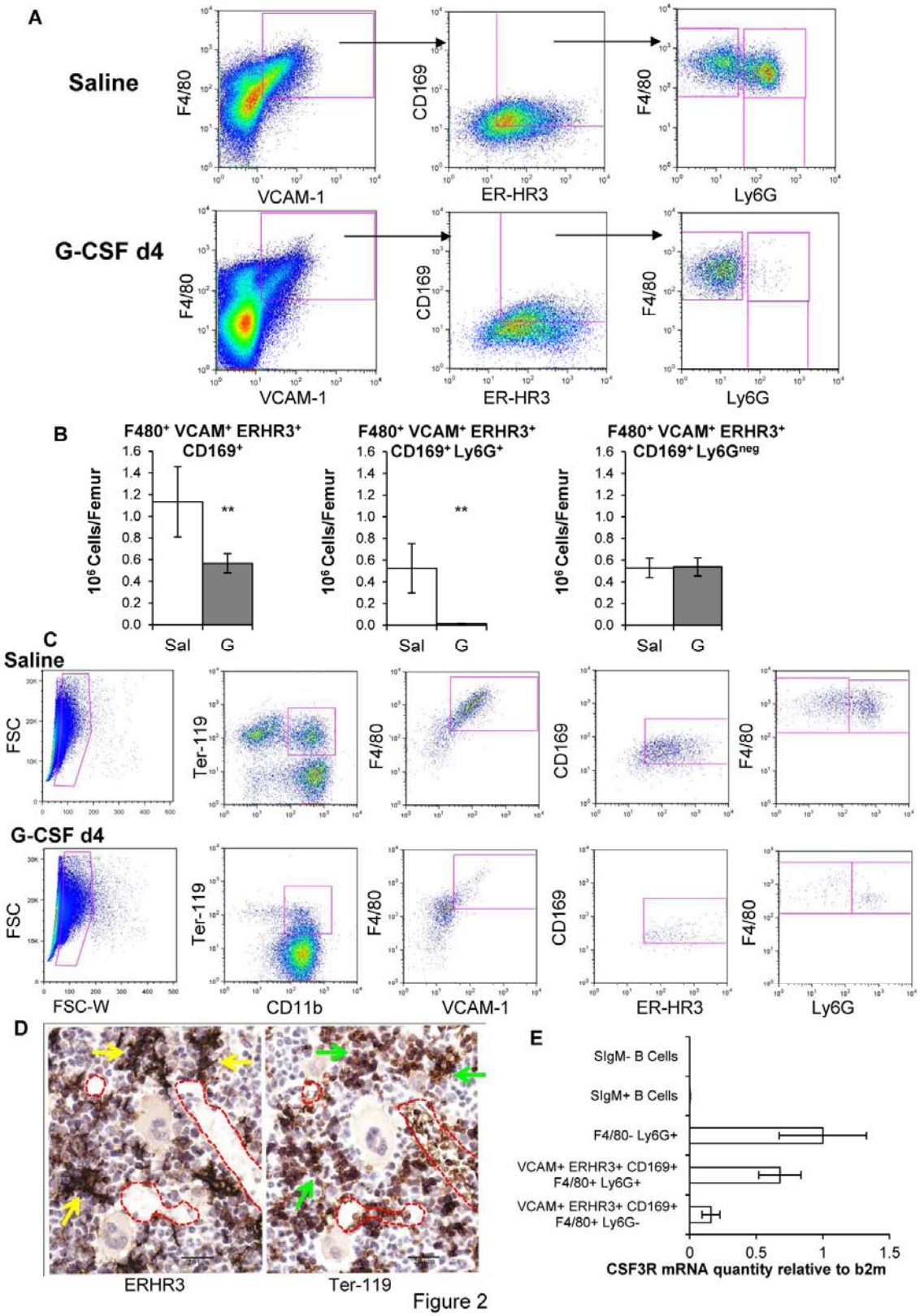
A
Saline
G-CSF d4
F4/80
VCAM-1
CD169
ER-HR3
Ly6G
B
F480+ VCAM+ ERHR3+ CD169+
F480+ VCAM+ ERHR3+ CD169+ Ly6G+
F480+ VCAM+ ERHR3+ CD169+ Ly6Gneg
10^6 Cells/Femur
Sal
G
**
C
Saline
G-CSF d4
FSC
FSC-W
Ter-119
CD11b
F4/80
VCAM-1
CD169
ER-HR3
Ly6G
D
ERHR3
Ter-119
E
SIgM- B Cells
SIgM+ B Cells
F4/80- Ly6G+
VCAM+ ERHR3+ CD169+ F4/80+ Ly6G+
VCAM+ ERHR3+ CD169+ F4/80+ Ly6G-
CSF3R mRNA quantity relative to b2m

Figure 2

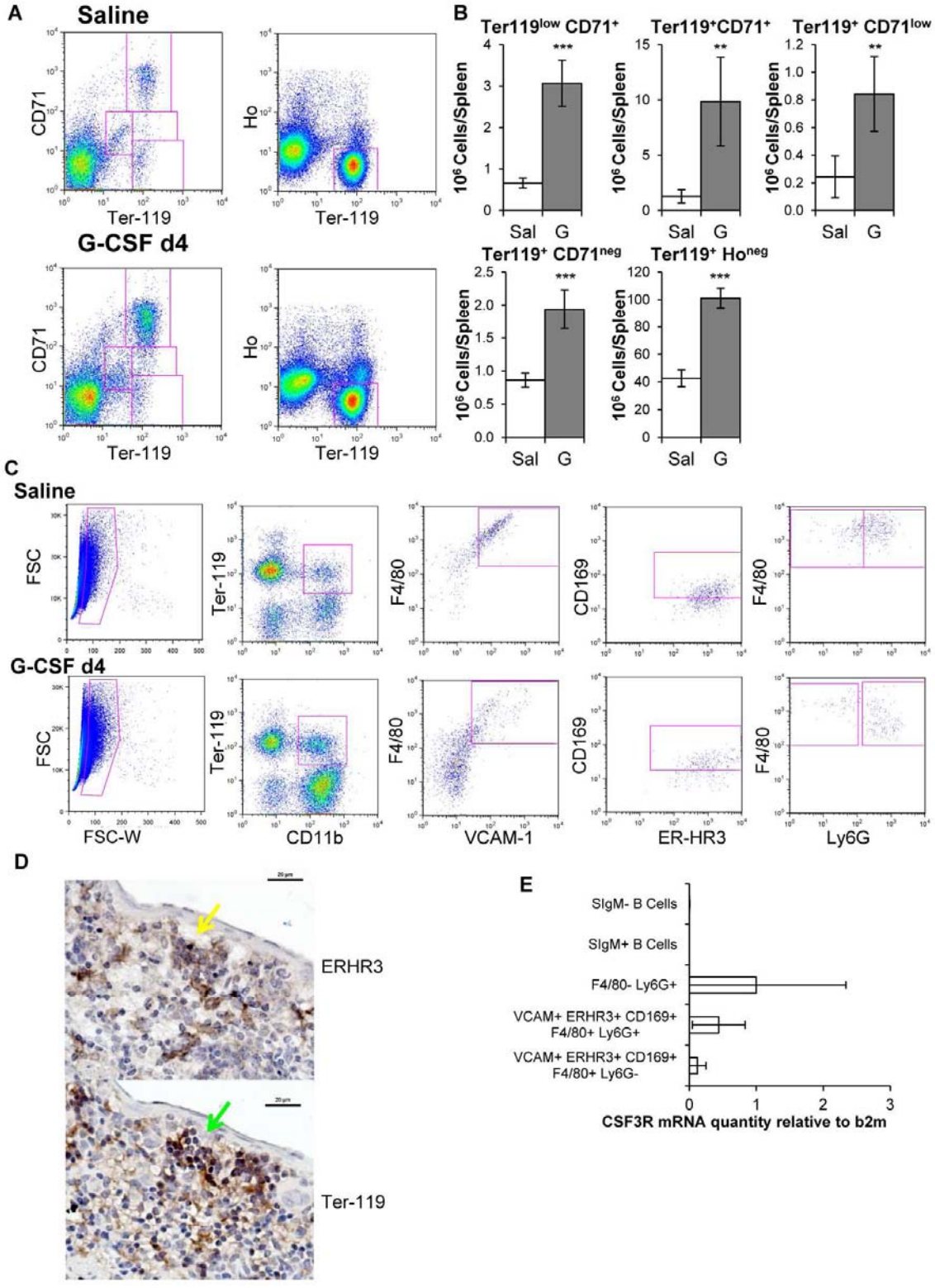
A
Saline
G-CSF d4
CD71
Ho
Ter-119
B
Ter119low CD71+
Ter119+CD71+
Ter119+ CD71low
Ter119+ CD71neg
Ter119+ Honeg
10⁶ Cells/Spleen
Sal
G
C
Saline
G-CSF d4
FSC
FSC-W
Ter-119
CD11b
F4/80
VCAM-1
CD169
ER-HR3
Ly6G
D
ERHR3
Ter-119
E
SIgM- B Cells
SIgM+ B Cells
F4/80- Ly6G+
VCAM+ ERHR3+ CD169+ F4/80+ Ly6G+
VCAM+ ERHR3+ CD169+ F4/80+ Ly6G-
CSF3R mRNA quantity relative to b2m

Figure 3

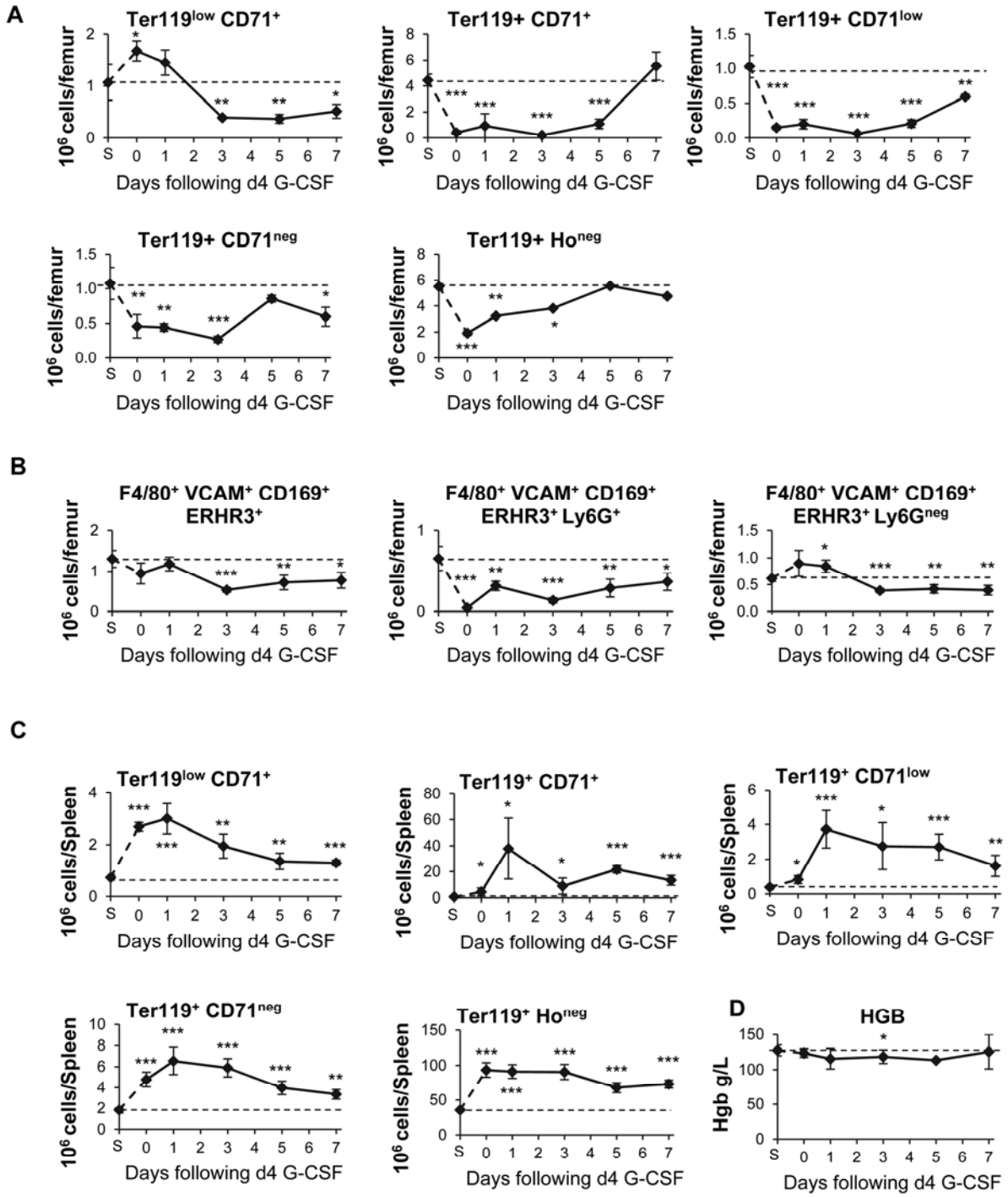
A
Ter119low CD71+
Ter119+ CD71+
Ter119+ CD71low
Ter119+ CD71neg
Ter119+ Honeg
10^6 cells/femur
Days following d4 G-CSF
B
F4/80+ VCAM+ CD169+ ERHR3+
F4/80+ VCAM+ CD169+ ERHR3+ Ly6G+
F4/80+ VCAM+ CD169+ ERHR3+ Ly6Gneg
C
Ter119low CD71+
Ter119+ CD71+
Ter119+ CD71low
Ter119+ CD71neg
Ter119+ Honeg
10^6 cells/Spleen
D
HGB
Hgb g/L

Figure 4

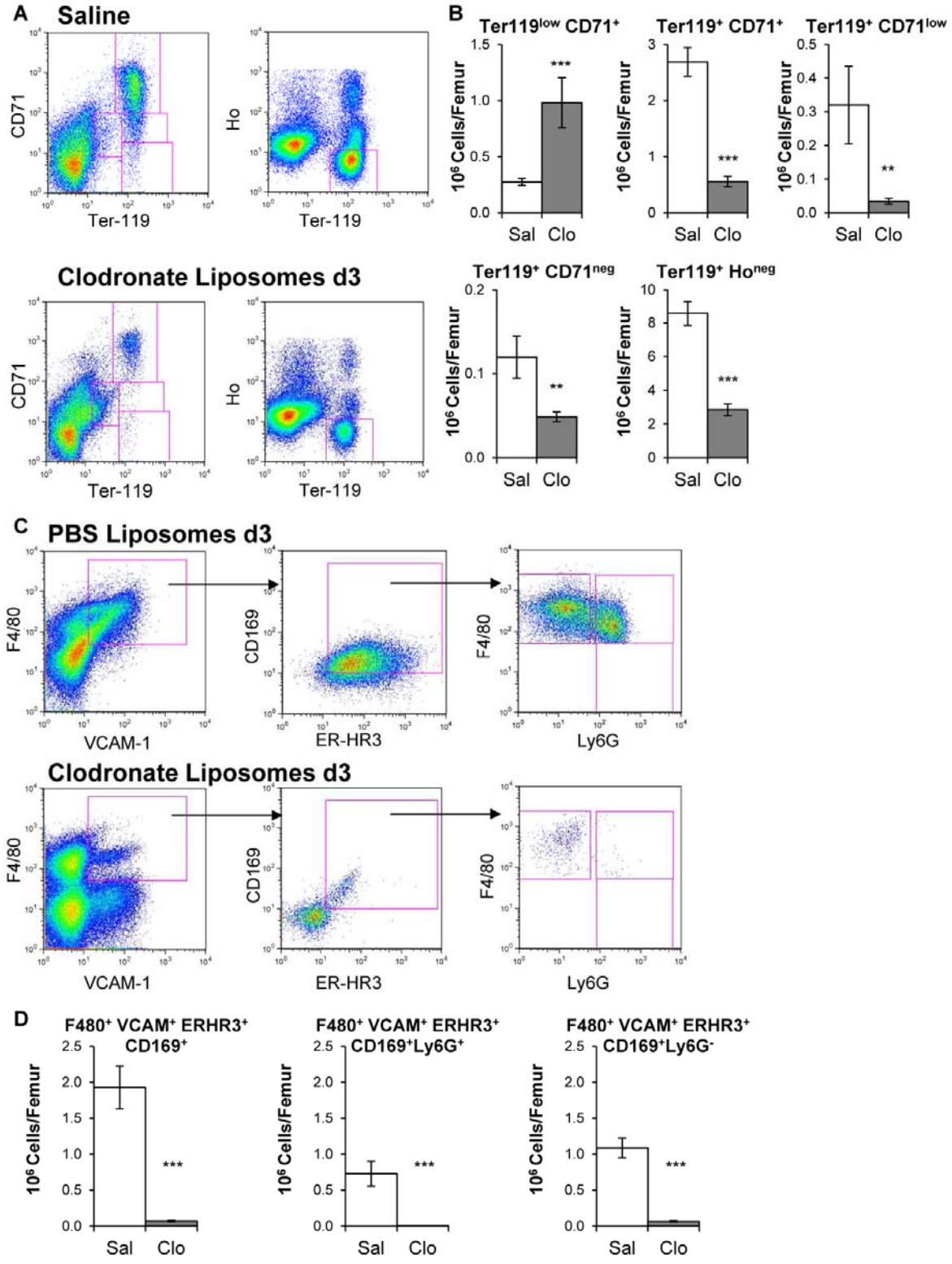
A
Saline
CD71
Ter-119
Ho
Ter-119
Clodronate Liposomes d3
CD71
Ter-119
Ho
Ter-119
B
Ter119low CD71+
Ter119+ CD71+
Ter119+ CD71low
Ter119+ CD71neg
Ter119+ Honeg
10⁶ Cells/Femur
Sal
Clo
***
**
C
PBS Liposomes d3
Clodronate Liposomes d3
F4/80
VCAM-1
CD169
ER-HR3
F4/80
Ly6G
D
F480+ VCAM+ ERHR3+ CD169+
F480+ VCAM+ ERHR3+ CD169+Ly6G+
F480+ VCAM+ ERHR3+ CD169+Ly6G-
10⁶ Cells/Femur
Sal
Clo

Figure 5

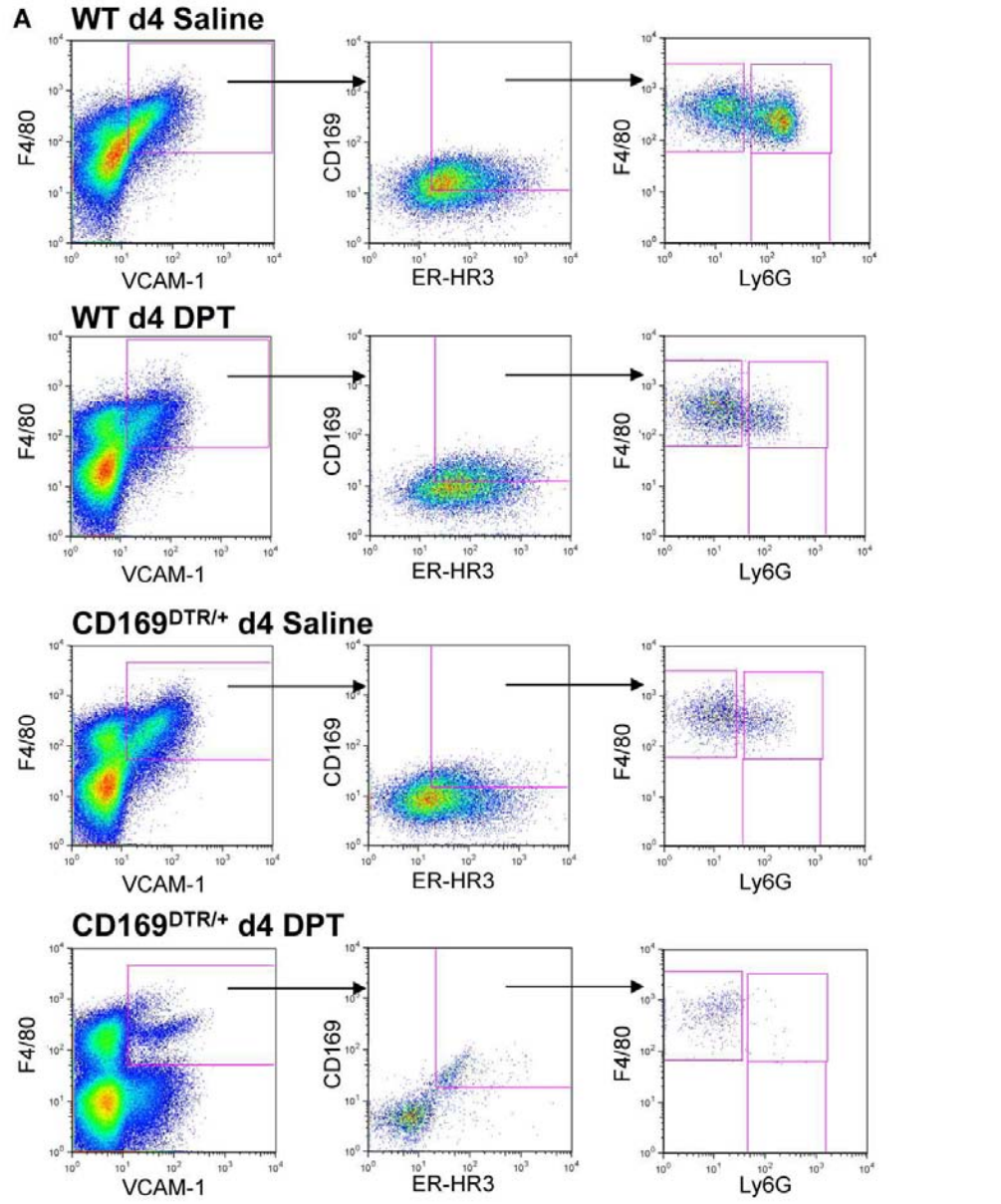
A
WT d4 Saline
WT d4 DPT
CD169DTR/+ d4 Saline
CD169DTR/+ d4 DPT
F4/80
VCAM-1
CD169
ER-HR3
Ly6G
B
F480+ VCAM+ ERHR3+ CD169+
F480+ VCAM+ ERHR3+ CD169+ Ly6G+
F480+ VCAM+ ERHR3+ CD169+ Ly6Gneg
Cells/Femur
600,000
500,000
400,000
300,000
200,000
100,000
0
***
**
DTR - + +
DPT + - +

Figure 6

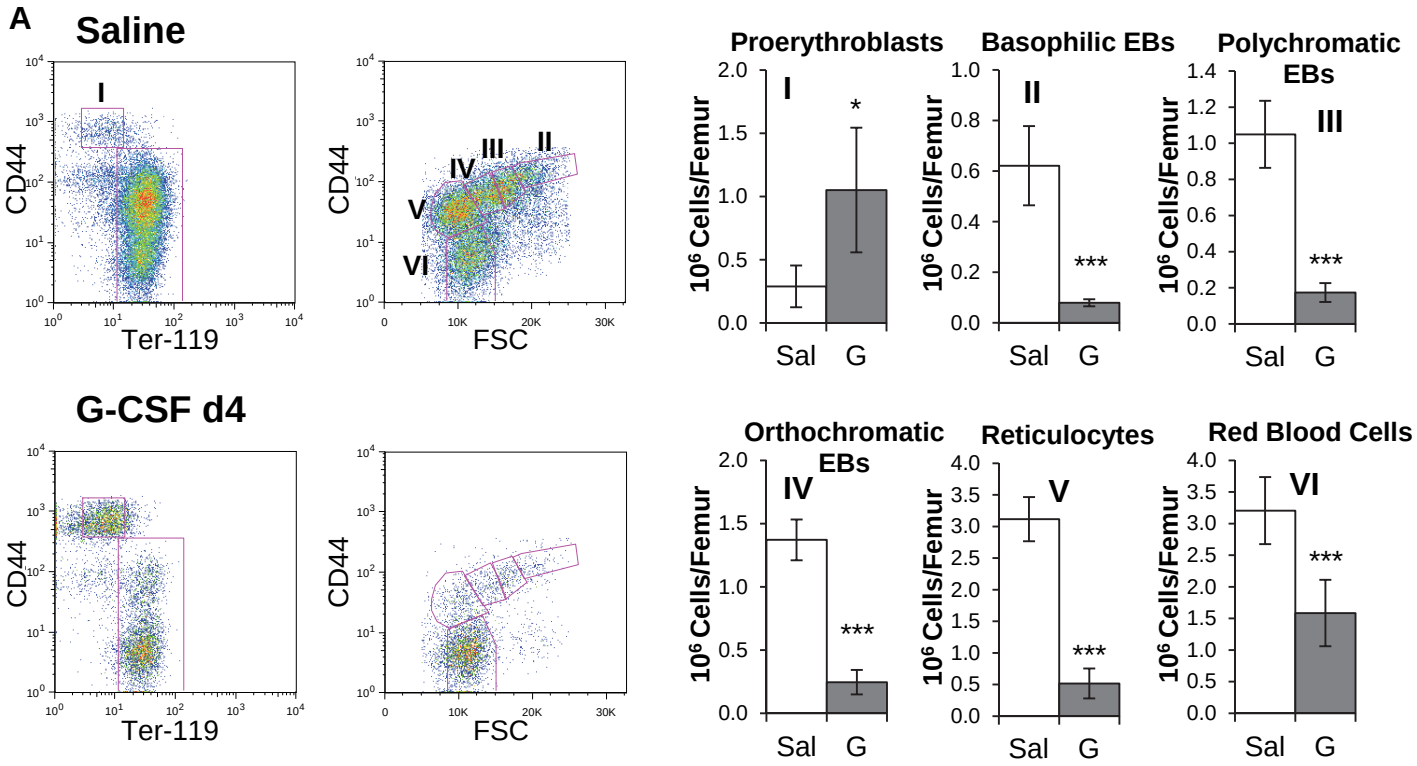

Supplementary Figure 1: G-CSF-mediated depletion of medullar erythropoiesis as measured with CD44, CD45 and Ter119 antibodies. (A) Representative flow cytometry dot-plots of mouse BM after a 4 day treatment with G-CSF or saline. The left dot-plots show Ter119 versus CD44 amongst gated CD45^{-} cells. Pro-erythroblasts were gated as Ter119^{low}CD44^{bright} (population I). Within the CD45^{-}Ter119^{+} population, basophilic erythroblasts (population II), polychromatic erythroblasts (population III), orthochromatic erythroblasts (population IV), reticulocytes (population V) and erythrocytes (population VI) were gated according to decreasing forward scatter and CD44 exporession. (B) Quantification of erythroid populations in the femoral BM after a 4 day course of saline (Sal) or G-CSF (G) treatment. n = 4 mice per group. Differences were evaluated with a t-test (* p≤0.05; ** p ≤ 0.01; *** p ≤ 0.001).

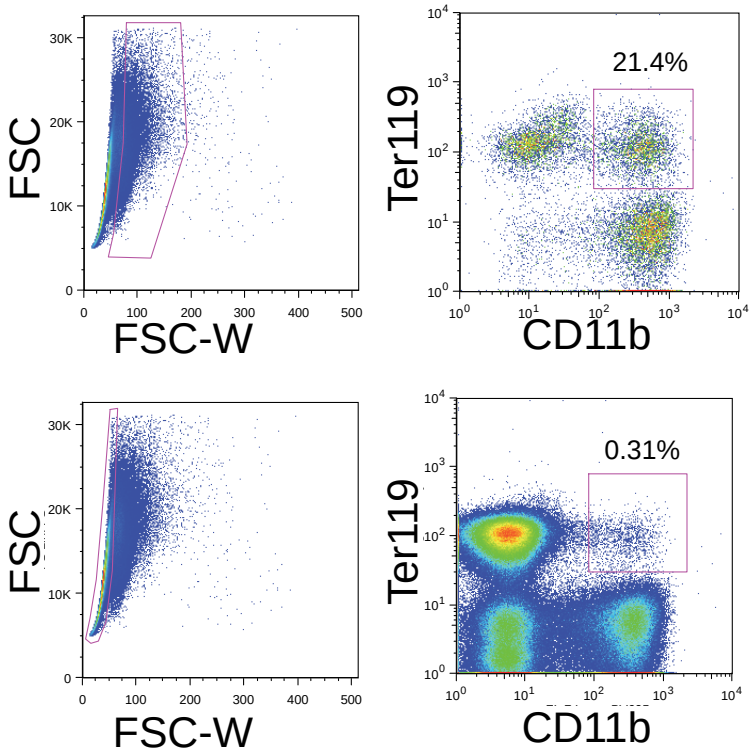

Supplementary Figure 2: Cells aggragates in the BM are enriched in clusters made of Ter119^{+} erythroid cells and CD11b^{+} myeloid cells. Representative phenotype of BM cell aggregates with high forward scatter peak width (in the top panels) and BM cell singlets with lower forward scatter peak width (in the lower panels) containing Ter119+ erythroid cells and CD11b+ myeloid cells. While 21% of cell aggregates in BM from saline-treated mice contain clusters of Ter119+ erythroid cells and CD11b+ cells, only 0.31% cells in the singlet gate contained Ter119+CD11b+ events.

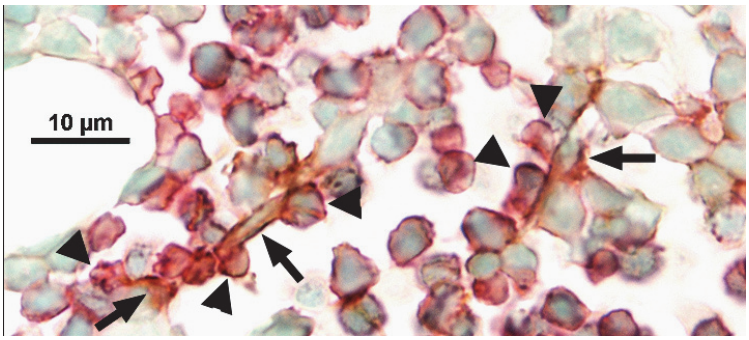

ER-HR3 (brown) **Ter-119 (red)**

Supplementary Figure 3: ER-HR3+ macrophages at the centre of erythoid islands. Double immunohistochemistry for ER-HR3 (brown) and Ter119 (red) antigens in femoral BM from from mice treated with saline. Reticulated ER-HR3+ macrophages are indicated by arrows at the center of clusters of Ter119+ erythroblasts (arrow heads).

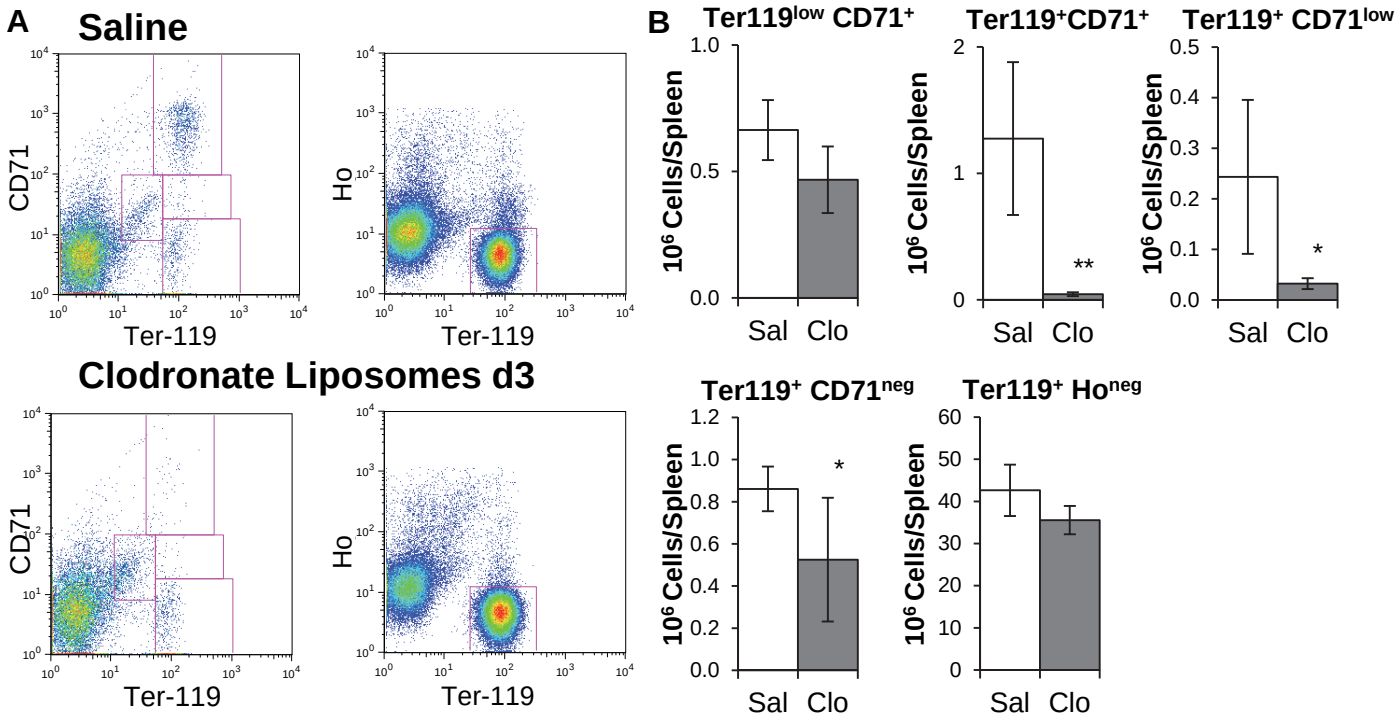

Supplementary Figure 4: Macrophage depletion with clodronate-loaded liposomes stops splenic erythropoiesis. (A) Representative flow cytometry dot-plots of spleens after a 3 day treatment with clodronate-loaded liposomes or saline. The left panels show Ter119 versus CD71 amongst Ho+ nucleated cells (Pro-erythroblasts were gated as Ter119lowCD71+, erythroblasts as Ter119+CD71+, polychromatic erythroblasts as Ter119+CD71low). In the right panel reticulocytes are gated as Ter119+ Ho-. (B) Quantification of erythroid populations in the spleen after a 3 day clodronate liposome (Clo) or saline (Sal) treatment. Data are mean ± SD of 4 mice per group from one representative experiment out of 2 independent repeats. Differences were evaluated with a t-test (* p≤0.05; ** p ≤ 0.01; *** p ≤ 0.001).

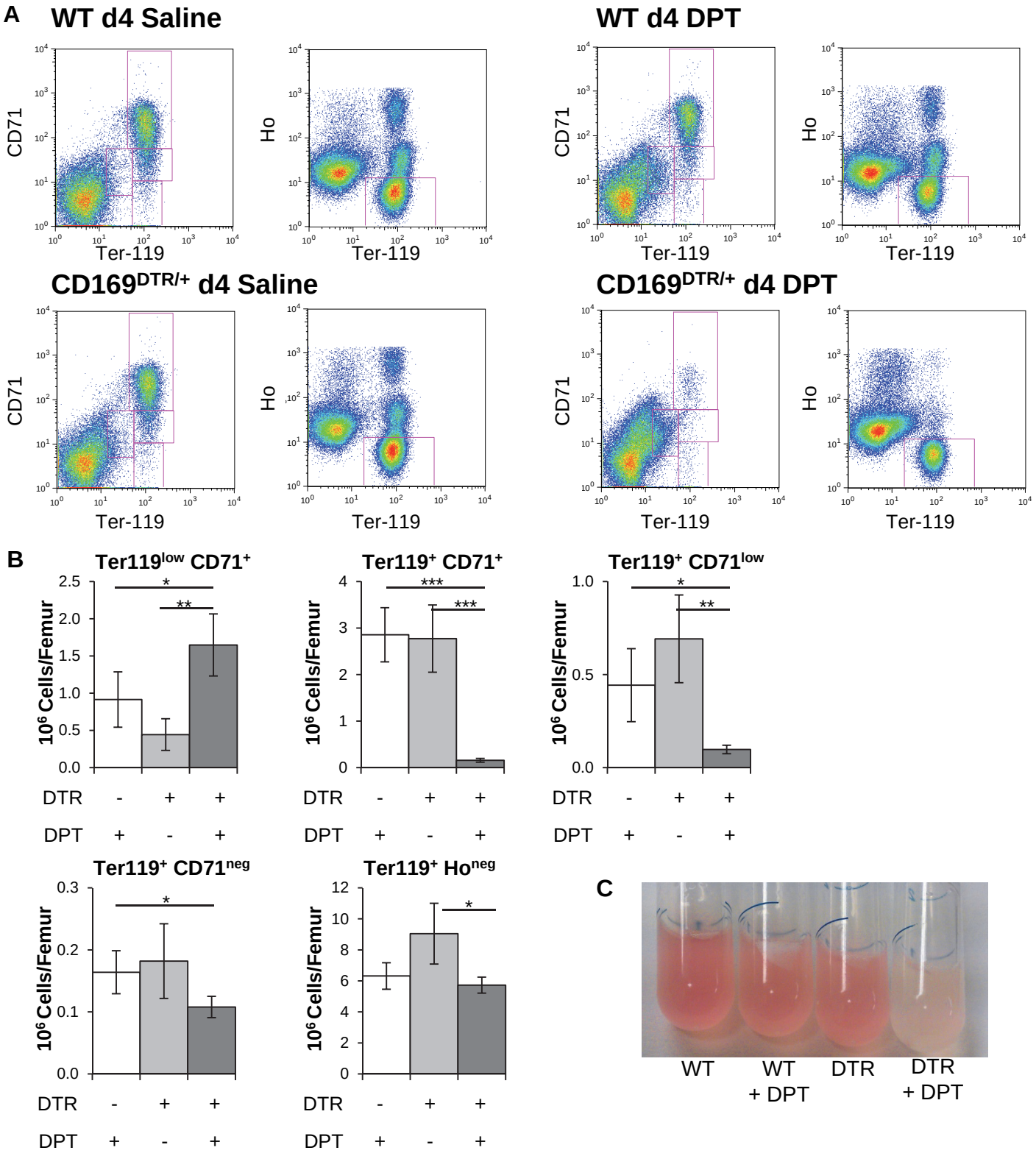

Supplementary Figure 5: Depletion of CD169⁺ macrophages stops medullary erythropoiesis. (A) Representative flow cytometry dot-plots of mouse BM after a 4 day treatment with saline or DPT in wild-type mice or *Siglec1*$^{DTR/+}$ mice. The left panels show Ter119 versus CD71 amongst Ho^{+} nucleated cells (Pro-erythroblasts were gated as Ter119^{low}CD71^{+}, erythroblasts as Ter119^{+}CD71^{+}, polychromatic erythroblasts as Ter119^{+}CD71^{low}). In the right panel reticulocytes are gated as Ter119^{+} Ho^{-}. (B) Quantification of erythroid populations in the femoral BM after a 4 day treatment with saline or DPT in wild-type mice or Siglec1$^{DTR/+}$ mice. DTR indicates the presence (+) or absence (-) of the *Siglec1*^{DTR} mutant allele. DPT indicates treatment with DPT (+) or saline (-). Data are mean ± SD of 4 mice per group from one representative experiment out of 2 independent repeats. Differences were evaluated with a t-test (* p≤0.05; ** p ≤ 0.01; *** p ≤ 0.001). (C) Photograph of mouse femoral BM flushed into 1 mL PBS after 4 day treatment with saline or DPT in wild-type and *Siglec1*$^{DTR/+}$ mice. Note the loss of red coloration following DPT treatment in *Siglec1*$^{DTR/+}$ mice.

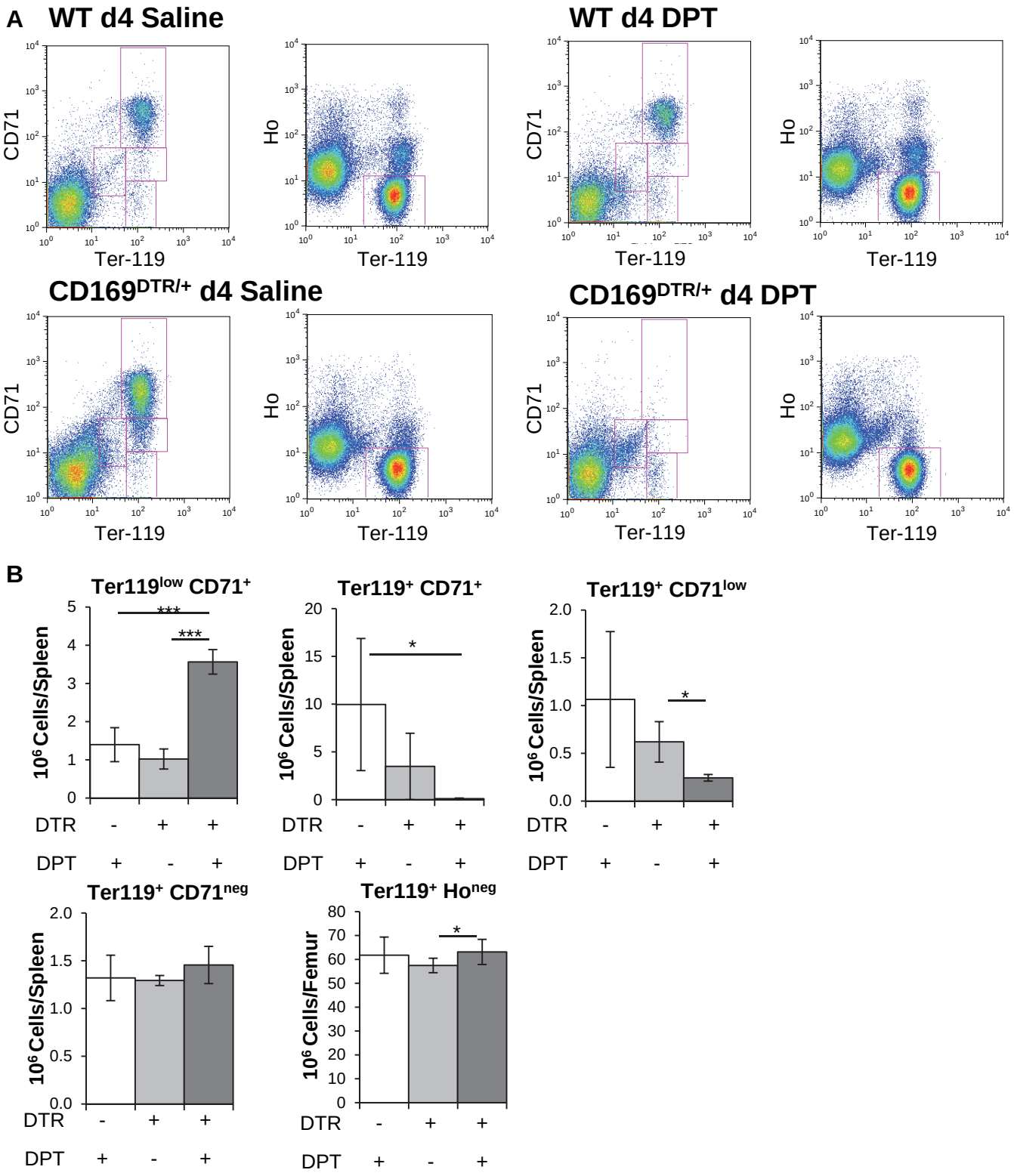

Supplementary Figure 6: Depletion of CD169+ macrophages stops splenic erythropoiesis. (A) Representative flow cytometry dot-plots of spleens after a 4 day treatment with saline or DPT in wild-type mice or *Siglec1*DTR/+ mice. The left panels show Ter119 versus CD71 amongst Ho+ nucleated cells (Pro-erythroblasts were gated as Ter119lowCD71+, erythroblasts as Ter119+CD71+, polychromatic erythroblasts as Ter119+CD71low). In the right panel reticulocytes are gated as Ter119+ Ho-. (B) Quantification of erythroid populations in the spleen after a 4 day treatment with saline or DPT in wild-type mice or Siglec1DTR/+ mice. DTR indicates the presence (+) or absence (-) of the *Siglec1*DTR mutant allele. DPT indicates treatment with DPT (+) or saline (-). Data are mean ± SD of 4 mice per group from one representative experiment out of 2 independent repeats. Differences were evaluated with a t-test (* p≤0.05; ** p ≤ 0.01; *** p ≤ 0.001).